People's Democratic Republic of Algeria

UNIVERSITY OF KASDI MERBAH OUARGLA

Faculty of New Technologies of Information and Communication

Department of Electronics and Telecommunications

FINAL STUDY DISSERTATION

In the aim of obtaining MASTER Degree – ACADEMIC

Domain: Science and Technology
Option: Automatic
Specialty: Automatic & System

Presented by:

OUMAYA MOHIEDDINE

BENRAS MOHAMED TAHAR

Topic

Predictive control of a mobile robot

Was Publicly Debated in: June 2018 in front of The Examining Committee Composed From:

Mr.	A. HAMZA	MAA	President	UKM Ouargla
Mr.	B. BENHELLAL	MAA	Supervisor	UKM Ouargla
Mr.	Y. RAHMANI	Doctorant	Co-Supervisor	UMSB Jijel
Ms.	F. KARA	MAA	Examiner	UKM Ouargla
Mr.	H. ELAGOUN	MAA	Examiner	UKM Ouargla

Academic year* : *2017 /2018

Acknowledgments

first and foremost, we must acknowledge our limitless thanks to Allah, the Ever-Magnificent. the Ever-Thankful to Allah, for His help us throughout our learning career. We are totally sure that this work would have never become truth, without His guidance.

We are grateful to some people, who worked with us from the beginning until the completion of the present research particularly our supervisor ***Mr. BENHELLAL Belkheir*** *and our Co-Supervisor* ***Mr. Rahmani Yacine****, We appreciate their efforts with us.*

We thank all the masters of the University of Ouargla, especially the masters of the department of electronics and communication.

We also extend our thanks to all our friends and colleagues especially those who bring us moral support, patience, an unforgettable and precious friendship.

Finally, we would like to thank all our families for their encouragement and unconditional support.

Thank you all…

OUMAYA Mohieddine

BENRAS Mohamed Tahar

DEDICATION

I dedicate this modest work to those who are the source of my inspiration and my courage.

To my dear mother, who always gives me hope to live and who has never stopped praying for me.

To my dear father, for his encouragement and support, And above all for his sacrifice so that nothing will hinder the course of my studies.

To all the professors and teachers who have followed me throughout my schooling and who have allowed me to succeed in my studies.

To my dear brother ***Ismail***

To my sisters ***asma ,hafsa*** *and* ***hind***

All my friends

#Benras mehamed tahar

To my dear mother which have always loved me unconditionally, and who has never stopped praying for me.

To my father Djamel, who, gives me confidence and always encouraged me;

In memory of my grandfather ***Madjid*** *and my grandmother;*

To my sister and my brother;

And to all relatives of my family ***oumaya*** *and* ***boughaba****;*

And to all who have taught me throughout my school life;

#Oumaya mohieddine

To all our dear friends and colleagues from the University of Ouargla:

S. Abd elmoula; A. Medab; S. Djamel; B. Riad; D. Djamel Eddine;

M. Romeyssa; H. Elmoundher; M. Khaled;

Contents

List of Figures

List of Tables

Symbols & Acronyms

AVG	Automated vehicle guided
DOF	Degree of freedom
GPS	Global Positioning System
UAVs	unmanned aerial vehicles
AUVs	autonomous underwater vehicles
LMRs	legged mobile robots
WMRs	wheeled mobile robots
RTAI	real-time application interface
GPC	Generalized Predictive Control
MPC	Model Predictive Control
PID	proportional–integral–derivative
SISO	single-input single-output
MIMO	multi-input-multi-output
NCGPC	Non-linear Continuous-time Generalized Predictive Control
δ_f	The front steering angle
δ_r	The rear steering angle
l_f	The longitudinal distance of the front tire
l_r	The longitudinal distance of the rear tire
I_z	The yaw-inertia moment
ψ	The yaw angle of vehicle in global axes

Symbols & Acronyms

$\dot{\psi}$	The yaw rate
$\ddot{y}$	The acceleration motion along the y axis
ρ	relative degrees
J	Quadratic criterion
β	Vehicle slip angle
c.g	center of gravity
α_y	The inertial acceleration of the vehicle at the c.g of the vehicle
C_f	The cornering stiffness of the front tire
C_r	The cornering stiffness of the rear tire
V_x	The longitudinal velocity at c.g. of vehicle
V_y	The lateral velocity at c.g.of vehicle (same as $\dot{y}$)
V_ψ	The yaw rate
M	The vehicle mass
fw	front wheels
rw	rear wheels
F_y^f & F_y^r	lateral tire forces of the front and the rear wheels respectively

General Introduction

Since the invention of the first robots, the field of robotics has witnessed many innovations and continuous developments, which is one of the most areas touched by rapid technological development.

Robots are considered a multi-disciplinary field, where including topics such as mechanics, mechatronics, electronics, automation, computer science, and artificial intelligence, robots have become an important part of our lives, where they are no longer a vision for the future but a reality of the present.

In robotics world, mobile robots get a special attention; this is due to their capability to navigate in their environment, where this feature allows it to perform a wide range of tasks. The contribution of mobile robots to the improvement of daily life and the tasks entrusted to them are endless, as they can touch all fields (e.g., unmanned aerial vehicles, independent underwater vehicles...etc.) [AGN08].

Mobile robot car-type is one of the most popular types of mobile robots because they are appropriate for typical applications. The movement of this type of robots is often controlled by determining the reference path to be followed, the problem of tracking the path is solved in a classical way by the kinematic model of the vehicle and this model is common because of it's simple structure and it's fine non-linear properties.

Outdoor mobile robots are exposed to natural obstacles that make the moving process hard, including off-road, wheel slippage at turns, difficult controlling at high speeds, These conditions make it impossible to dispense with the dynamic model that takes all these characteristics into account, so the controller relies on the dynamic model in the control process.

The dynamic control of skid-steering robots was studied in particular in [LCI99] using a dynamic feedback linearization paradigm for a model-based controller which minimizes lateral skidding by imposing the longitudinal position of the instantaneous center of rotation. Another algorithm reported in [KP04], offers a good robustness considering uncertainties on the robot dynamic parameters. Some studies have addressed this point, mainly by considering sliding as a perturbation of a nominal model (kinematic or assuming constant grip conditions). Such a perturbation is then rejected using robust control approaches, such as those proposed in [LCO02] while [ELB08] acts differentially on each wheel speed to reduce the influence of sliding on the global robot dynamics.

Predictive control techniques are one of the advanced technologies in the science of

automation, the idea of expectation is often linked to the concept of prophecy: to say what will happen tomorrow according to what is happening today and what happened yesterday. From this concept, the predictive control techniques were created, which rely on the use of a model, in order to predict the behavior of a system that is controlled by a number of constraints.

The real starts of this method were only in the early 1980s thanks to the work of D. Clarke, but this control technology attracted industrial attention in the late 1970s. What makes this one of the most powerful control law is not it's ability to take account of current and future dynamics (the expected situation) and only potential constraints, but this technology can be also applied to multi-input and multi-output systems, and linear or nonlinear systems [BOU11].

The dynamic characteristics of the outdoor mobile robot make it difficult to control. Because these characteristics directly affect the controller, a good path tracking of a non-linear dynamic system (outdoor mobile robot car-type), is not achievable through classical controllers, the NCGPC is an ideal solution for the problem of tracking trajectory, as well as its ability to handle system changes smoothly and without complicated procedures.

In this work, we are looking forward to controlling a trajectory tracking by applying The Non-linear continuous-time generalized prediction control (NCGPC) approach to the outdoor mobile robot car-type model.

In order to reach this goal, this dissertation will be divided into four chapters:

The first chapter contains an overview of robotics, as well as a detailed presentation of the mobile robots and their main components, In addition, a description of the concerned robot in this work.

The second chapter the mathematical development of both kinematic and dynamic models of lateral movement of the vehicle will be provided.

The third Chapter provides a detailed explanation of predictive control, the principle of work and the philosophy based on it, and presents the mathematical development for the nonlinear continuous-time generalized predictive control (NCGPC) approach in the case of a multi-input-multi-output system.

The fourth Chapter present test results of applied non-linear continuous-time generalized predictive control (NCGPC) approach in the model of the mobile robot car type, and analysis of these results, in addition, contains the results of the performance test and its analysis. We will conclude with a general conclusion and propose some perspectives for the future continuation of this work.

Chapter I

Overview of Mobile Robots

I.1 Introduction

Robots have played a very important role in human daily life nowadays, which it becomes difficult to dispense to them; this is due to their facilitation to daily life hard tasks, or repetitive tasks.

Mobile robots are one of the most important robots types, which their importance lie in their ability to move in many areas, thus provide solutions to many problems that was existed, (heavy things transfer, Space exploration trips, etc.).

This kind of mobile robot has been developed many times in all its types, including the ground mobile robots, which is the focus of our interest, where we will deal with a mobile robot vehicle type.

In this chapter, we set a general definition of robotics, the classification of all robot types, and the focus on mobile robots with their principal component.

I.2 General definition

A robot is defined as a mechanical or virtual agent, controlled by a computer program or other electronic circuitry. Autonomy, either fully or partly, is a prerequisite to the definition of a robot.

This can range from a machine that simply mimics humanoid or lifelike movements to the concept of fully realized robots that have intelligence or self-awareness. The branch of science and technology dealing with the concept, design, construction, and implementation of robots is robotics. The word "robot" it self originates from the Czech language meaning, "forced labor." It was first coined by Czech playwright Karel Capek in 1921.The first robots were developed by William Gray Walter in England in the late 1940s, and in 1961 robots were used by General Motors to lift heavy metal parts in the factory to avoid risks to human workers. Since then, robots have been applied to the main aspects of modern society, in the industrial field, and the most difficult tasks or environments hostile to humans, such as space, deep sea or in combat [KC15].

I.3 Robots types

There are many classifications of robot types, which are categorized according to their applications, size and function.

In this work, we classed robot types into two large parts, fixed-base robots (manipulators) and mobile robots.

I.3.1 Manipulateurs

A manipulator can be defined as a mechanism usually composed of a series of slides, or sliding to each other, for the purpose of absorption and transition Objects are usually an enzymatic degree of freedom. Remote control may be by computer or human. There are several types of armor, each type has its uses, including spherical manipulator, Cylindrical manipulators and so on [San99].

Fig. I.1: manipulator robot arm

Fig. I.2: OMRON manipulator robot

I.3.2 Mobile robots

Mobile robots are robots that can move from one place to another autonomously, that is, without assistance from external human operators. Unlike the majority of industrial robots that can move only in a specific workspace, mobile robots have the special feature of moving around freely within a predefined workspace to achieve their desired goals. This mobility capability makes them suitable for a large repertory of applications in structured and unstructured environments. Ground mobile robots are distinguished in wheeled mobile robots (WMRs) and legged mobile robots(LMRs) Mobile robots also include unmanned aerial vehicles (UAVs), and autonomous underwater vehicles(AUVs) [Tza14].

I.4 History of mobile robots

The Turtle built by Gray Walter in the year 1950, is one of the first autonomous mobile robots. Gray Walter uses only a few analog components, including vacuum tubes, but his robot is able to move towards a light that marks a goal, to stop in front of obstacles and recharge his batteries when he arrives in his niche figure (I.3).

All these functions are performed in a fully prepared environment but remain basic functions that are still research and technological development topics to make them more and more generic and robust [FIL16].

Fig. I.3: The Turtle of Gray Walter in 1950

In the 60s, research electronics will lead, with the appearance of the transistor, a more complex robots, but will perform similar tasks.

Thus, the "Beast" robot Fig (I.4) of John Hopkins University is able to move in the center of the corridors using ultrasonic sensors, look for electrical outlets (black on white walls) using photo-diodes and to recharge.

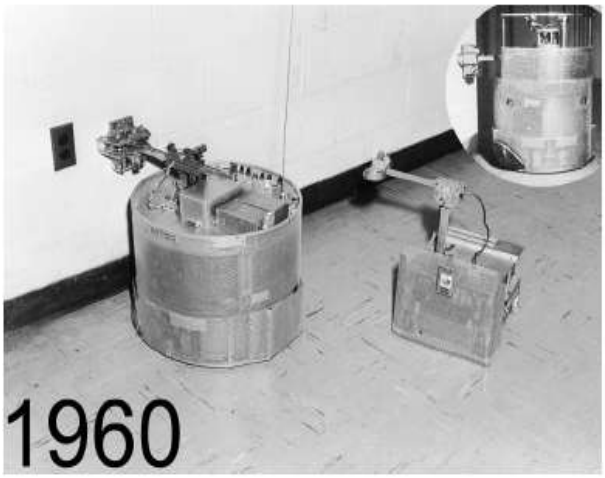

Fig. I.4: Robot "Beast" from John Hopkins University in the 1960s

The first links between artificial intelligence research and robotics appeared in Stanford in 1969 with Shakey Fig (I.5).

This robot uses ultrasonic rangefinders and a camera and serves as a platform for artificial intelligence research, which at the time was essentially working on symbolic approaches to planning [FIL16].

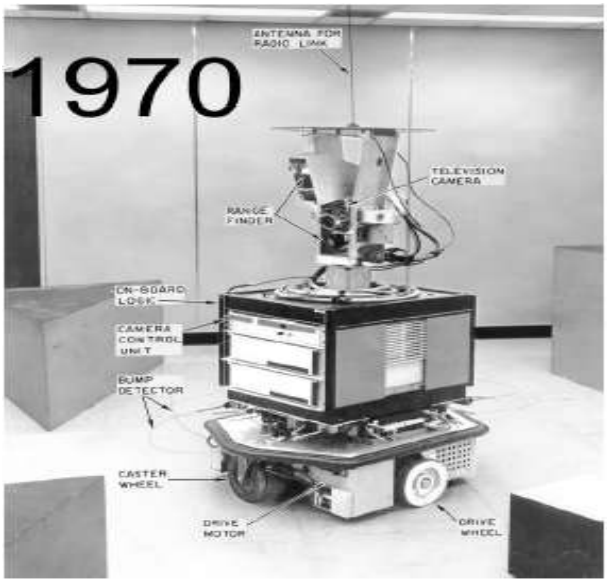

Fig. I.5: The Stanford Shakey robot in 1969,The artificial intelligence research platform

The perception of the environment, which at the time is considered as a separate problem, even secondary, is particularly complex and leads here to strong constraints on the environment.

These developments continue with Stanford Cart in the late 1970s, including the first uses of stereo-vision for obstacle detection and environmental modeling Fig (I.6).

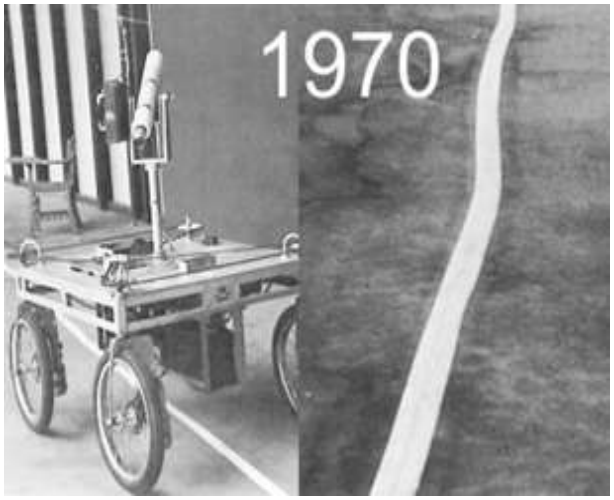

Fig. I.6: The Stanford Cart, 1970s

In France, the Hilare robot is the first robot built at LAAS, in Toulouse Fig (I.7).

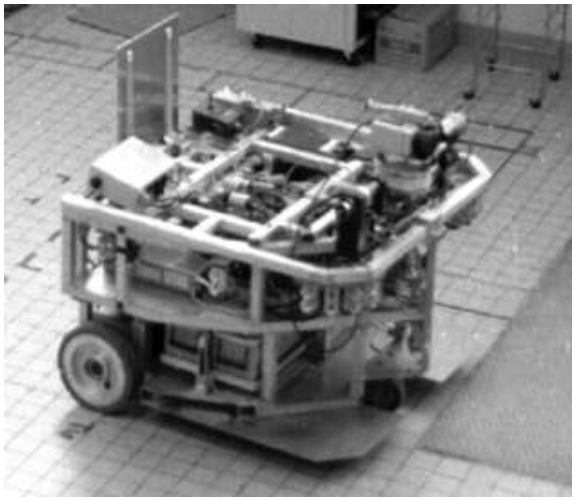

Fig. I.7: The Hilare robot LAAS, built in 1977

Fig. I.8: Genghis, developed by Rodney Brooks at MIT in the early 1990s

An important milestone in the early 1990s with the emphasis on reactive robotics, represented in particular by Rodney Brooks. This new approach to robotics, which puts perception at the center of the problem, has made it possible to go from very large, very slow robots to small robots Fig (I.8), which are much more responsive and adapted to their environment [FIL16].

These robots use little or no modeling of the world, a problem that has proven to be extremely complex.

These developments have continued and the arrival on the market since the 1990s of integrated platforms such as the pioneer of the company Mobile Robots has allowed many laboratories to work on mobile robotics and led to an explosion of diversity of research themes. Thus, even if the problems of displacement in space and modeling of the environment remain difficult and crucial, for example, laboratories have been able to work

on multi-robot approaches, the problematic of learning or the problems of interactions between humans and robots [FIL16].

I.5 types of mobile robots

The types of mobile robots according to their working environment can be divided into three sections.

I.5.1 Underwater Robots

Camera-equipped underwater robots serve many purposes including tracking of fish and searching for sunken ships [Sol07].

Fig. I.9: Underwater Robots

I.5.2 Flying Robots

Flying robots have been used effectively in military maneuvers, and often mimic the movements of insects [Sol07].

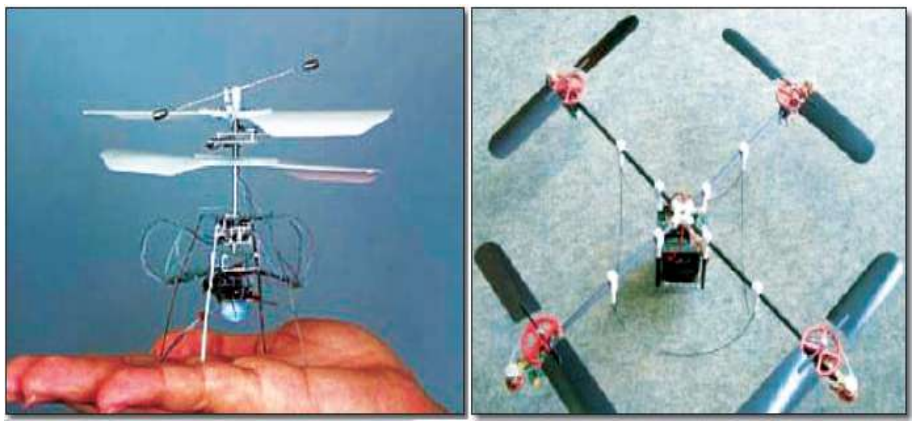

Fig. I.10: Flying robots

I.5.3 Ground Robot

Locomotion of ground mobile robots is distinguished in:

❶ **Legged locomotion:** Legged robots are distinguished in two main categories:

❶ **.a. Two-legged (bipedal) robots:** Bipedal locomotion is standing on two legs, walking and running [Tza14].

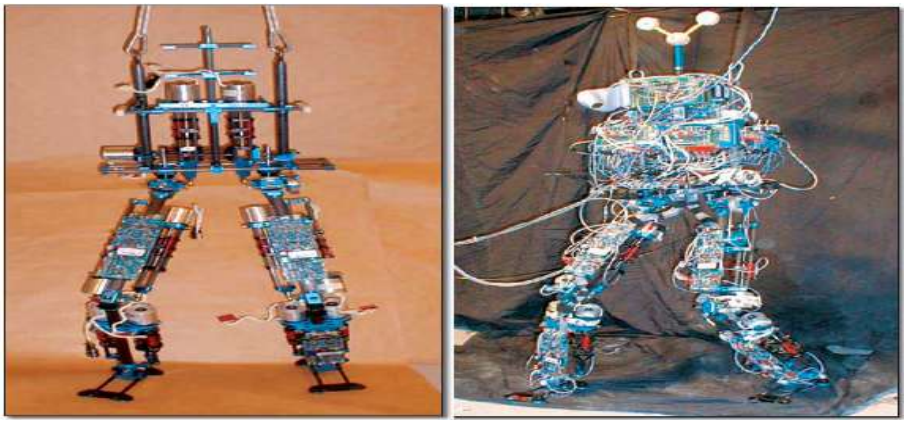

Fig. I.11: M2, a 3D bipedal walking robot

❶ **.b. Many-legged robots:** The multi-legged robots are inspired by the animals, in this kind of robot for statically stable walking, the minimum duty factor needed is three (number of legs), where three is the minimum number of feet in on-state to assure static stability. A walking gait is one where at least one foot is on the ground at any time [Tza14].

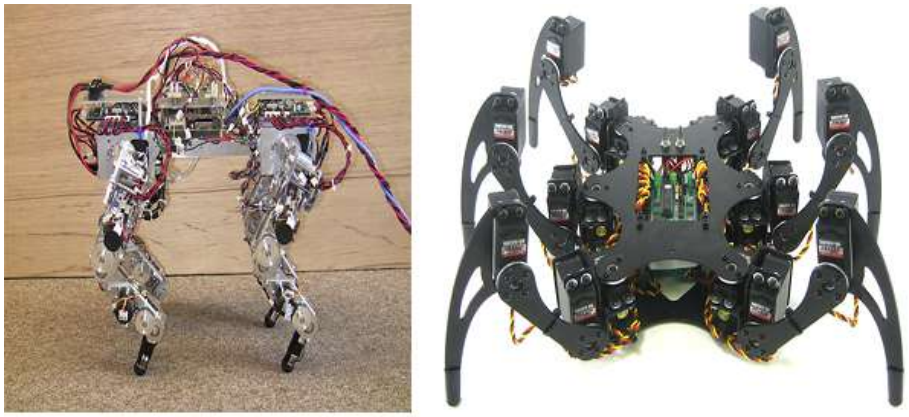

Fig. I.12: The quadruped robo"Kotetsu" & Robo-spider

❷ **Wheeled Locomotion:** The maneuverability of a WMR depends on the wheels and drives used. The WMRs that have three DOF are characterized by maximal maneuverability which is needed for planar motions, such as operating on a warehouse floor, a road, a hospital, a museum, etc. Nonholonomic WMRs have less than three DOF in the plane, but they are simpler in construction and cheaper because less than three motors are used. A holonomic vehicle can travel in every direction

and function in tight areas. This capability is called omnidirectionality. Balance is inherently assured in WMRs with three or more wheels. But in the case of m-wheel WMRs ($m \geq 3$) a suspension system must be used to assure that all wheels can have ground contact in rough terrains. The main problems in WMR design are the traction, maneuverability, stability, and control that depend on the wheel types and configurations (drives) [Tza14].

I.6 Classification of wheeled mobile robot (WMRS)

We present quickly the classification of the wheels used in the different types of mobile bases (platforms) in robotics.

I.6.1 Differentially Driven WMRs

Differential drive configuration is the most common wheeled mobile robot configuration. It is used because of its simplicity and versatility. It is the easiest to implement and to control. A differentially driven WMR consists of two driving wheels and one or two castor wheels. In a differentially driven WMR, the relative motion of the two driving wheels with respect to each other achieves the required motion. The caster wheels are used just to support the structure. The motion of a differentially driven WMR is simple. The straight-line motion is attained in the robot when the two driving wheels rotate at the same speed. Motion in the reverse direction is achieved by the rotation of the wheels in the opposite direction. Turning is achieved by braking one wheel and rotating the other. The robot rotates about the fixed wheel. Sharp turning can be attained by rotating both the wheels in opposite directions. Motion along an arc can be attained by the differential motion of both the wheels with respect to each other [Sol07].

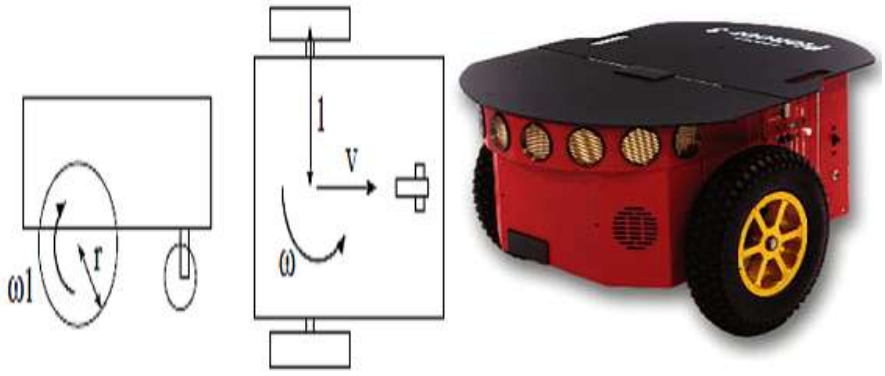

Fig. I.13: Differentially driven robot

I.6.2 Omnidirectional WMRs

Omnidirectional movement of WMRs is of great interest for complete maneuverability. This kind of wheel configuration imposes no kinematic constraint on the robot chassis. Hence, the robot can freely change it's direction at any instant. The odometry solution for

this configuration is done in a similar fashion to that for differential drive, with position and velocity data derived from the motor (or wheel) shaft encoders. Figure (I.14) explains the wheel configuration for two such wheel configurations. The fixed standard wheel steered standard wheel, or castor wheels cannot achieve omnidirectional motion [Sol07].

There are two different wheel configurations to achieve omnidirectional movement:

✠ Swedish Wheel

✠ Spherical Wheel

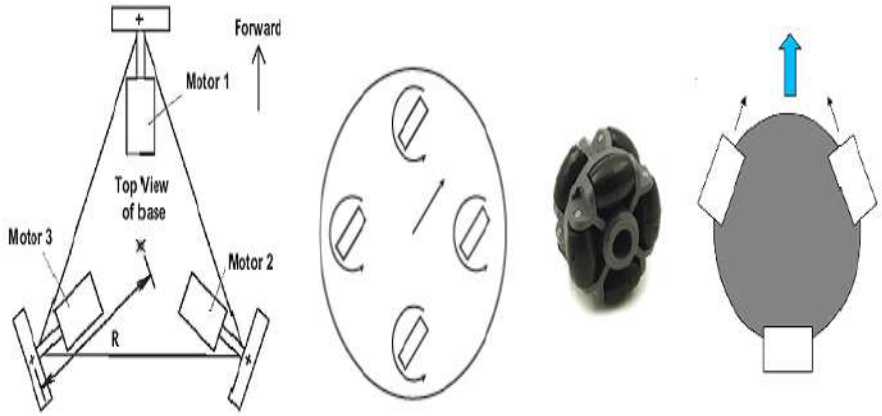

Fig. I.14: omnidirectional wheel

I.6.3 Synchro Drive WMRs

An innovative configuration known as synchro drive features three or more wheels mechanically coupled in such a way that all rotate in the same direction at the same speed, and similarly pivot in unison about their respective steering axes when executing a turn. This drive and steering "synchronization" results in improved odometry accuracy through reduced slippage, since all wheels generate equal and parallel force vectors at all times [Sol07].

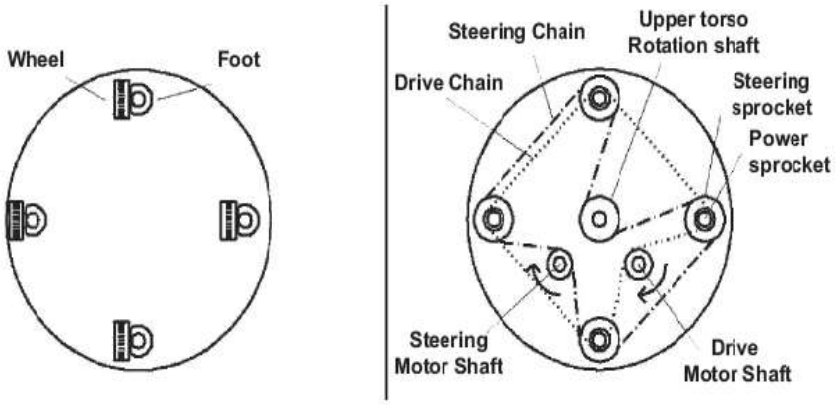

Fig. I.15: A four-wheel syncro-drive configuration: Bottom view and Top view

I.6.4 Car-type WMRs

Car-type configurations (see Figure I.16) employing one (tricycle-drive) or two driven front wheels and two passive rear wheels (or vice versa) are fairly common in AVG applications because of their inherent simplicity. One problem associated with the tricycle-drive configuration is that the vehicle's center of gravity tends to move away from the front wheel when traversing up an incline, causing a loss of traction. Ackerman steering provides a fairly accurate odometry solution while supporting the traction and ground clearance needs of the all-terrain operation. Ackerman steering is thus the method of choice for outdoor autonomous vehicles [Sol07].

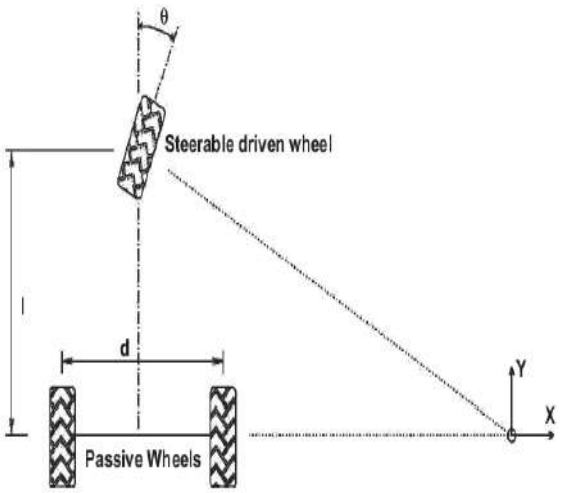

Fig. I.16: Tricycle-driven configurations

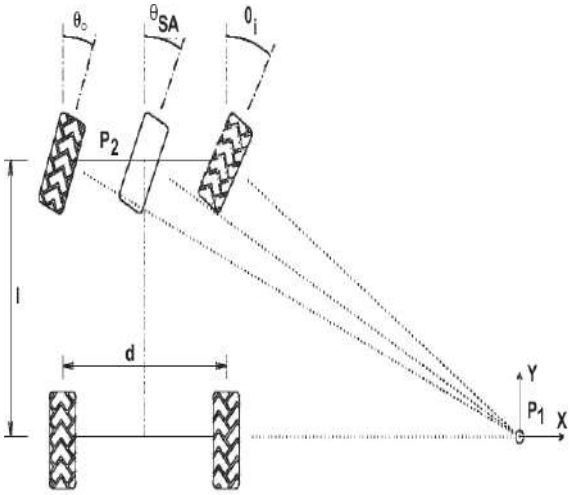

Fig. I.17: Ackerman-steered vehicle,

I.7 Description of the RobuFast-A platform

The model used in this work is a mathematical model of an experimental platform, called RobuFast-A, shown in figure (I.18), is a robot with independent four-wheel drive, and two Ackerman type steering gear. It is designed to reach the speed of $10m/s$, the platform has 4 independent suspensions with double wishbones and equipped with oleo-pneumatic shock absorbers (without spring).

The main characteristics of the robot are given in the table (I.1). The location of the robot uses a differential GPS (Real-Time Kinematics RTK) brand Magellan Proflex 500 ($20Hz$, accuracy 2cm according to x, y and $5cm$ according to z). The yaw angle of the vehicle is estimated thanks to an inertial unit XsensMTi brand ($0,1deg/s$ gyroscope accuracy). Two coders optics are installed for the measurement of the front and rear steering angles [Kri12].

The wheels are operated independently thanks to 4 geared motors encoders and directly integrated into the wheels.

Table I.1: RobuFast-A settings

Description	value
Front wheel-base l_f	*0.625 m*
Rear wheel-base l_r	*0.575 m*
Half – way e	*0.4 m*
Height h	*0.9 m*
Mass M	*420 kg*
Wheel radius r	*0.25 m*
Mass of wheels M_w	*3 kg*

The control of the robot is possible manually through the low-level PC which manages the reactive controls requiring very short sampling times.

On this PC operating under the Linux operating system RTAI, libraries of Aroccam software architecture are used for allowing the acquisition of data and their dating. Another PC is used for the implementation of control and observation algorithms [Kri12].

Fig. I.18: The RobuFast-A experimental platform

I.8 Sensors

All sensors used in mobile robotics provide information belonging to one of two broad categories of information: proprioceptive information and exteroceptive information [FIL16].

I.8.1 proprioceptive sensors

Proprioceptive sensors allow a measurement of the robot's movement. These are the sensors that can be used most directly for localization, but they suffer from a drift over time that generally does not allow them to be used alone:

❉ Odometry

❉ Doppler and optical radar systems

❉ Inertial systems [FIL16]

I.8.2 Exteroceptive sensors

The exteroceptive information links the robot with his environment strongly, which provide information about the movement of the robot and his position in its environment there are two major categories it is used in the mobile robots, Rangefinders and Cameras [FIL16].

Rangefinders:

There are different types of rangefinders, which measure the distance to the elements of the environment, using various physical principles [FIL16]:

- Ultrasonic rangefinders
- Infrared rangefinders
- Laser rangefinders

Cameras:

The use of a camera to perceive the environment is an attractive method because it seems close to the methods used by humans and provides a large amount of information on the environment. However, the processing of the large and complex data provided by these sensors is often difficult, but it is a highly researched and promising avenue of research for robotics [FIL16]:

- Simple cameras
- Stereoscopic cameras
- Panoramic cameras

Other sensors:

We can also find in Exteroceptive sensors other kinds of sensors, which it doesn't belong to camera's kind or to rangefinder's kind [FIL16]:

- Touch sensors
- Tags(marks)
- GPS

I.9 Conclusion

In this chapter, we presented a general definition of robotics with their classifications. We highlighted mobile robots in particular and presented their classifications and their most important elements.

The purpose is to choose the type of robot that will deal with in the rest of this work, and the target robot is a mobile robot car type with four wheels, where a mathematical model will be in the next chapter.

Chapter II

The Kinematic & The Dynamic Model of The Lateral Movement of The Vehicle

II.1 Introduction

The individuals need to deal with all issues of the world around them; these needs lead to create tools and systems to help with that. In the industrial world, the direct dealing with machines and robots could be a real obstacle to engineers and researchers. Mathematical models provided ideal solutions for such problems. It has become easy to know the behavior of many systems and their changes by presenting them in a mathematical model that describes their behavior in best way.

The mathematical model will be used in this work in order to understand the behavior of the mobile robot type car, this model will make it easier for us to deal with this system later.

In this chapter, we will introduce the model of the lateral movement of the vehicle and introduce a dynamic model that describes the dynamic behavior of the vehicle comprehensively.

II.2 kinematic model of lateral vehicle motion

The kinematic model for the lateral motion of a vehicle based on certain assumption whish described below , this model provide a mathematical description of the vehicle motion without taken the force that effect the motion in consideration.

consider a bicycle model of the vehicle as shown in the figure (II.1), In this model, instead of using two front wheels we should use only one to present the two in the center of the wheel at the point A, the same thing with the rear wheels which changed into a signal wheel in center at the point B , steering angle of the front and rear wheels are presented by δ_f and δ_r respectively [Raj12] .

By the assumption that taken in this model, both front and rear wheels can be steered ,the center of the gravity (c.g) of the vehicle is at the point C. the distance between c.g and the point A is denoted by l_f and between c.g and the point B is denoted by l_r.

The vehicle is assumed to have planar motion. Three coordinates are required to describe the motion of the vehicle: X,Y and ψ.(X, Y) are inertial coordinates of the location of the c.g. of the vehicle while describes the orientation of the vehicle. The velocity at the c.g. of the vehicle is denoted by V and makes an angle β with the longitudinal axis of the vehicle. The angle β is called the slip angle of the vehicle [Raj12].

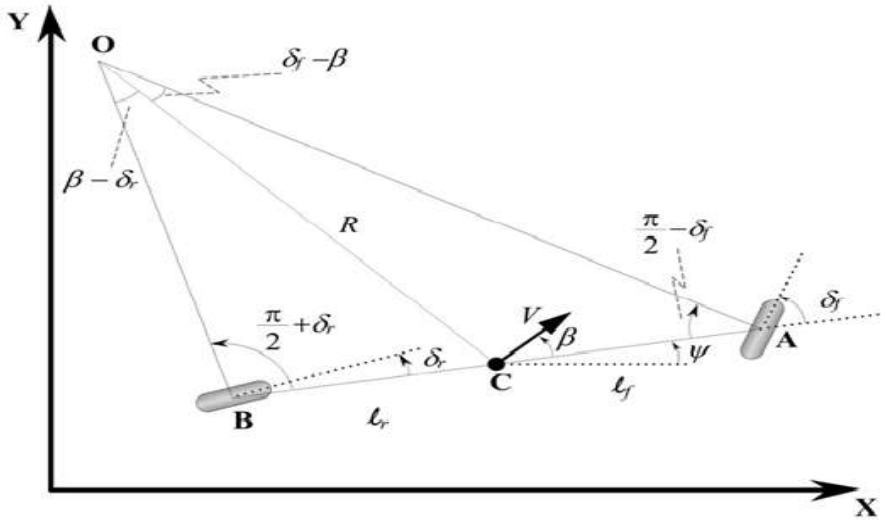

Fig. II.1: Kinematics of lateral vehicle motion

♣ **Assumption:**

In a kinematic model ,the major assumption is that the velocity vector in the point A and B are In the orientation direction of the front and the rear respectively , which means the slip angles of the front and rear wheels are zero ,the assumption is reasonable for low speed motion of the vehicle [Raj12] ,

At the low speed the lateral force for both wheels with a circular path with radius R is $\sum f_y = \frac{mv^2}{R}$

Point O, instantaneous center of orientation is defined by the intersection of OA lines and OB, these two lines are perpendicular to the orientation of the front and rear wheels successively [Raj12].

- The vehicle trajectory radius defined by the line OC.
- The center of gravity velocity is perpendicular to OC.
- Apply the sine rule to triangle OCA.

$$\frac{\sin(\delta_f - \beta)}{l_f} = \frac{\sin(\frac{\pi}{2} - \delta_f)}{R} \tag{II.1}$$

Apply the sine rule to triangle OCB.

$$\frac{\sin(\beta - \delta_r)}{l_r} = \frac{\sin(\frac{\pi}{2} + \delta_r)}{R} \tag{II.2}$$

From.Eq (II.1)

$$\frac{\sin(\delta_f)\cos(\beta) - \sin(\beta)\cos(\delta_f)}{l_f} = \frac{\cos(\delta_f)}{R} \tag{II.3}$$

From.Eq (II.2)

$$\frac{\cos(\delta_r)\sin(\beta) - \cos(\beta)\sin(\delta_r)}{l_r} = \frac{\cos(\delta_r)}{R} \tag{II.4}$$

Multiply both sides of Eq.(II.3) by $\frac{l_f}{\cos(\delta_f)}$ we get:

$$\tan(\delta_f)\cos(\beta) - \sin(\beta) = \frac{l_f}{R} \tag{II.5}$$

Multiply both sides of Eq. (II.4) by $\frac{l_r}{\cos(\delta_r)}$ we get:

$$\sin(\beta) - \tan(\delta_r)\cos(\beta) = \frac{l_r}{R} \tag{II.6}$$

Adding Eqs. (II.5) and (II.6)

$$\{\tan(\delta_f) - \tan(\delta_r)\}\cos(\beta) = \frac{l_f + l_r}{R} \tag{II.7}$$

The change of vehicle orientation $\dot{\psi}$ is equal to the vehicle angular velocity $\frac{V}{R}$,so:

$$\dot{\psi} = \frac{V}{R} \tag{II.8}$$

Using Eq. (II.7) and Eq.(II.8) can be re-written as

$$\dot{\psi} = \frac{V\cos(\beta)}{l_f + l_r}(\tan(\delta_f) - \tan(\delta_r)) \tag{II.9}$$

The overall equations of motion are therefore given by:

$$\dot{X} = V\cos(\psi + \beta) \tag{II.10}$$

$$\dot{Y} = V\sin(\psi + \beta) \tag{II.11}$$

$$\dot{\psi} = \frac{V\cos(\beta)}{l_f + l_r}(\tan(\delta_f) - \tan(\delta_r)) \tag{II.12}$$

where$(\psi + \beta)$,the course angle representing the angle between the longitudinal axis X and the velocity vector of the vehicle V [Raj12].

The slip angle can be obtained by multiplying Eq. (II.5) by l_r and subtracting it from Eq. (II.6) multiplied by l_f :

$$\beta = \tan^{-1}\left(\frac{l_f\tan\delta_r + l_r\tan\delta_f}{l_f + l_r}\right) \tag{II.13}$$

Table II.1: summary of kinematic model equations

summary of kinematic model equations		
Symbol	**Nomenclature**	**Equation**
X	*Global X axis coordinate*	$\dot{X} = V\cos(\psi + \beta)$
Y	*Global Y axis coordinate*	$\dot{Y} = V\sin(\psi + \beta)$
ψ	*Yaw angle; orientation angle of vehicle with respect to global X axis*	$\dot{\psi} = \frac{V\cos(\beta)}{l_f + l_r}(\tan(\delta_f) - \tan(\delta_r))$
β	*Vehicle slip angle*	$\beta = \tan^{-1}\left(\frac{l_f\tan\delta_r + l_r\tan\delta_f}{l_f + l_r}\right)$

[Raj12]

♣ Simulation results

the velocity vector at the front steering wheel makes an angle δ_f with the longitudinal axis of the vehicle. Likewise, the velocity vector at the rear steering wheel makes an angle δ_r with the longitudinal axis of the vehicle.

We have a constant speed $(V_x = 10m/s)$
We choose the angles with the same value $\delta_f = \delta_r = 0.3$ We get the results of the simulation that shown in the following figure:

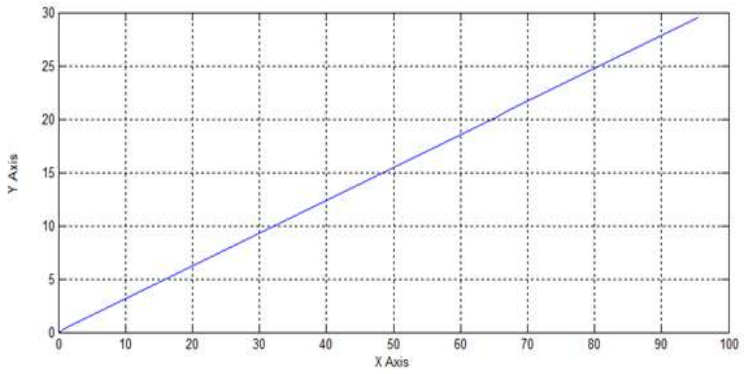

Fig. II.2: Vehicle trajectory for $\delta_f = \delta_r = 0.3$

we give a certain value to the front steering angle and we set the rear steering angle at zero $\delta_f = 0.3$, $\delta_r = 0$, $(V_x = 10m/s)$ and we get as a simulation results :

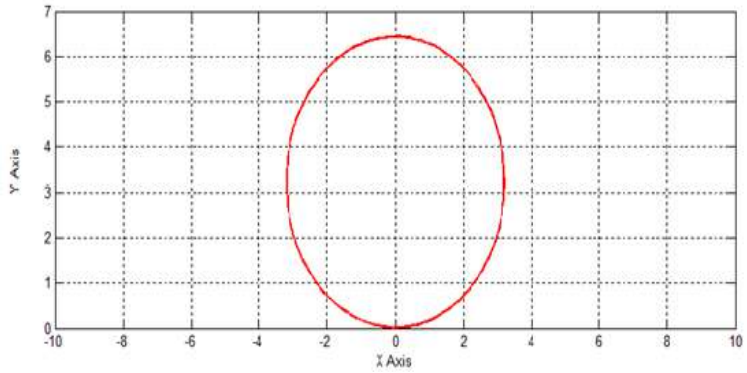

Fig. II.3: Vehicle trajectory for $\delta_f = 0.3/\delta_r = 0$

II.3 Dynamic lateral model

The kinematic model can no longer be used in the higher vehicle speed, and with taken into account the dynamic vehicle's parameters mass, inertia, as well as tire contact conditions on the ground [Ben10].

The dynamic model can be so complicated to deal with, unless we take into account the following assumptions that can make it affordable :

• The vehicle is moving at a constant speed .

• The movement of the pitch and poll doesn't taken into consideration .

• the suspension characteristic aren't taken into consideration .

• The dynamic movement of the vehicle is described by two references which one of them is a fix reference (O,X,Y,Z) and the other a mobile reference which set on the center of gravity of the vehicle(O, X,Y,Z) [Ben10].

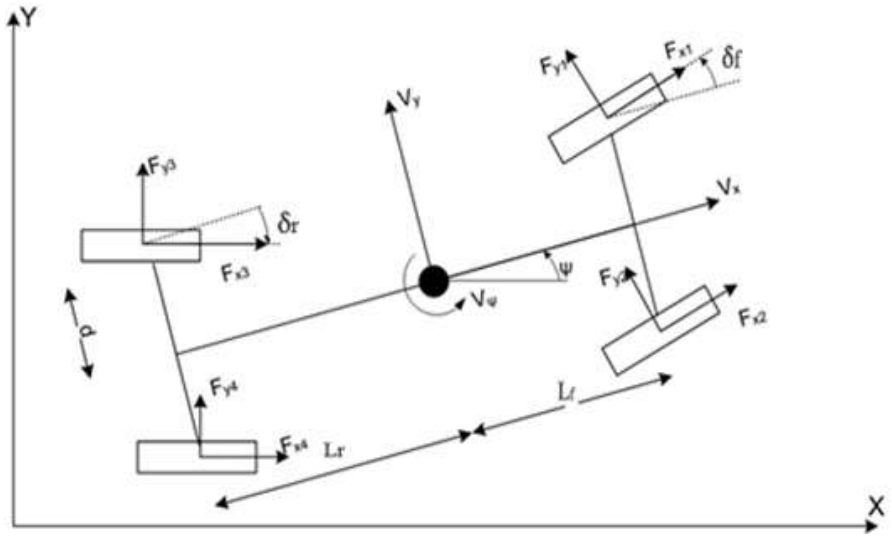

Fig. II.4: Model of the four-wheeled mobile robot

II.4 Dynamic modeling of the lateral movement of the vehicle

The equations of the dynamic model which describe the movement of the vehicle are given either by the method of Lagrange, or by the laws of Newton in this work we will use Newton's laws which defined as:

The sum of the external forces applied to a solid body moving in a given direction, is equal to the product of the mass by acceleration in that direction [Raj12].

$$m\alpha_y = F_y^f + F_y^r \tag{II.14}$$

• α_y = The inertial acceleration of the vehicle at the c.g of the vehicle.

• F_y^f and F_y^r = lateral tire forces of the front and the rear wheels respectively.

since the movement of the yaw of the vehicle is taken into account so $\alpha_y \neq \ddot{y}$,but it will written in this way $\alpha_y = \ddot{y} + V_x\dot{\psi}$

• $\ddot{y}$ = The acceleration motion along the Y axis.

• $\dot{\psi}$ = The yaw rate.

✠ By changing the actual value of α_y in the Newton's lows we get :

$m(\ddot{y}+V_x\dot{\psi}) = F_y^f + F_y^r$ The sum of the torsion moments on a given axis is equal to the product of inertia and the acceleration of rotation along this axis [Raj12].

$$I_z\ddot{\psi} = l_f F_y^f - l_r F_y^r \tag{II.15}$$

• I_z = The yaw-inertia moment
• l_f = The longitudinal distance of the front tire from the c.g. of the vehicle.
• l_r = The longitudinal distance of the rear tire from the c.g. of the vehicle.

II.5 The drift angle of the wheels

The angle of drift of the wheels due to the tires are soft, they deform under the action of the forces exerted laterally, so that when crossing a corner, the wheels being deflected in a given direction, the vehicle tends to move along a slightly different trajectory.

This slight difference between the directionally imposed steering by the steering wheel and the real direction of the vehicle is called the drift angle α [Ben10].

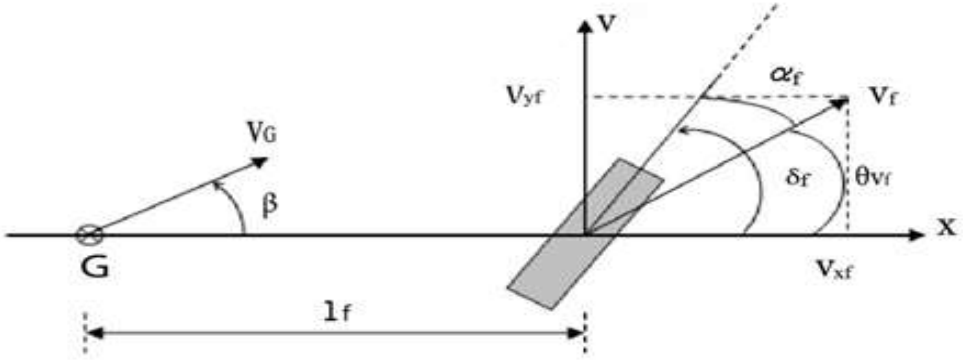

Fig. II.5: Angle of drift of the front wheel

The drift angles of the front and rear wheels is given by :

$$\alpha_f = \delta_f - \theta_{vf} \tag{II.16}$$

$$\alpha_r = \delta_r - \theta_{vr} \tag{II.17}$$

• δ = Is the front wheel steering angle.

• θ_v = The angle that the velocity vector makes with the longitudinal axis of the vehicle, and it can be given after linear approximation by [Raj12]:

$\tan(\theta_{vf}) = \frac{V_y + \dot{\psi} l_f}{V_x} \rightarrow \theta_{vf} = \tan^{-1}(\frac{V_y + \dot{\psi} l_f}{V_x}) \approx \theta_{vf} = \frac{V_y + \dot{\psi} l_f}{V_x}$ and the same thing with the rear wheel.

which $\theta_{vr} \approx \frac{V_y + \dot{\psi} l_r}{V_x}$

By applicating Newton's lows we get :

$$\dot{\alpha}_y = \dot{V}_y + V_x \dot{\psi}$$

$$m\dot{\alpha}_y = m(\dot{V}_y + V_x \dot{\psi}) = 2F_y^f \cos(\delta_f) + 2F_x^f \sin(\delta_f) + 2F_y^r \cos(\delta_r) + 2F_x^r \sin(\delta_r) \quad \text{(II.18)}$$

$$\dot{\alpha}_x = \dot{V}_x - V_y \dot{\psi}$$

$$m\dot{\alpha}_x = m(\dot{V}_x - V_y \dot{\psi}) = 2F_x^f \cos(\delta_f) - 2F_y^f \sin(\delta_f) + 2F_x^r \cos(\delta_r) - 2F_y^r \sin(\delta_r) \quad \text{(II.19)}$$

In order to study the lateral control of our vehicle, we need a model which faithfully represents the lateral dynamics, in this case the longitudinal behavior is neglected, that is to say when the speed is a constant, that the longitudinal forces are zero, we obtain the following model [Ben10]:

$$m(\dot{V}_y + V_x \dot{\psi}) = 2F_y^f \cos(\delta_f) + 2F_y^r \cos(\delta_r) \approx 2F_y^f + 2F_y^r \quad \text{(II.20)}$$

From Eq. (II.20) we get:

$$\dot{V}_y = \frac{2F_y^f}{m} + \frac{2F_y^r}{m} - V_x \dot{\psi} \quad \text{(II.21)}$$

The lateral tire force for the wheels of the vehicle can be written as [Ben10] :

$$F_y^{(f,r)} = C^{(f,r)} \alpha^{(f,r)}$$

$$F_y^f = C_f(\delta_f - \theta_{vf}) \quad \text{(II.22)}$$

$$F_y^r = C_r(\delta_r - \theta_{vr}) \quad \text{(II.23)}$$

where C_f and C_r define the cornering stiffness of the front and rear tires of the vehicle. These depend on wheel / ground adherence conditions and rheological properties of the tire [Ben10].

By replacing Eq.(II.22) and (II.23) in Eq.(II.21) we get:

$$\dot{V}_y = \frac{2C_f}{m}\left[\delta_f - \frac{V_y + \dot{\psi} l_f}{V_x}\right] - \frac{2C_r}{m}\left[\delta_r - \frac{V_y - \dot{\psi} l_r}{V_x}\right] - V_x V_\psi$$

$$\dot{V}_y = \frac{-2(C_f + C_r)}{mV_x} V_y + \left[-\frac{-2(C_f l_f - C_r l_r)}{mV_x} - V_x \right] V_\psi + \frac{2C_f}{m}\delta_f + \frac{2C_r}{m}\delta_r \tag{II.24}$$

$$I_z \ddot{\psi} = l_f F_{y_f} - l_r F_{y_r} \tag{II.25}$$

By replacing Eq.(II.22) and (II.23) in Eq.(II.24) we get:

$$I_z \dot{V}_\psi = 2l_f C_f \left[\delta_f - \frac{V_y + \dot{\psi} l_f}{V_x} \right] - 2l_r C_r \left[\delta_r - \frac{V_y + \dot{\psi} l_r}{V_x} \right]$$

$$\dot{V}_\psi = \left[\frac{-2C_f l_f + 2C_r l_r}{I_z V_x} \right] V_y + \left[-\frac{2C_f l_f^2 + 2C_r l_r^2}{I_z V_x} \right] V_\psi + \frac{2C_f l_f}{I_z}\delta_f - \frac{2C_r l_r}{I_z}\delta_r \tag{II.26}$$

from the equation (II.9) and (II.10) the representation of state space of our system can be written as:

$$\begin{bmatrix} \dot{V}_y \\ \dot{V}_\psi \end{bmatrix} = A \begin{bmatrix} V_y \\ V_\psi \end{bmatrix} + B \begin{bmatrix} \delta_f \\ \delta_r \end{bmatrix}$$

✓which:

$$A = \begin{bmatrix} \frac{-2(C_f + C_r)}{mV_x} & -\frac{-2(C_f l_f - C_r l_r)}{mV_x} - V_x \\ \frac{-2C_f l_f + 2C_r l_r}{I_z V_x} & -\frac{2C_f l_f^2 + 2C_r l_r^2}{I_z V_x} \end{bmatrix}$$

$$B = \begin{bmatrix} \frac{2C_f}{m} & \frac{2C_r}{m} \\ \frac{2C_f l_f}{I_z} & -\frac{2C_r l_r}{I_z} \end{bmatrix}$$

✓With $\begin{bmatrix} V_y \\ V_\psi \end{bmatrix}$ the state vector, and the model inputs are the lateral velocity at c.g.of vehicle V_y and the yaw rate V_ψ .

In this project, we are looking forward to get the trajectory tracking as results, for this reason we support the dynamic model with a kinematic model, the state space is enhanced with the orientation ψ and the robot absolute position (X; Y) of the robot in an absolute frame R. The trajectory to be followed is defined as a collection of successive coordinates expressed in the same absolute frame [Ben10].

$$\dot{x} = V_x \cos(\psi) + V_y \sin(\psi)$$

$$\dot{y} = V_x \sin(\psi) + V_y \cos(\psi)$$

$$\dot{\psi} = V_\psi$$

Table II.2: summary of Dynamic model equations

summary of Dynamic model equations		
Symbol	**Nomenclature**	**Equation**
V_y	*The lateral velocity at c.g. of vehicle (same as $\dot{y}$)*	$\dot{V}_y = A_{11}V_y + A_{12}V_\psi + B_{11}\delta_f + B_{12}\delta_r$
V_ψ	*The yaw rate*	$\dot{V}_\psi = A_{21}V_y + A_{22}V_\psi + B_{21}\delta_f + B_{22}\delta_r$
ψ	*The yaw angle of vehicle in global axes*	$\dot{\psi} = V_\psi$
X	*Global X axis coordinate*	$\dot{x} = V_x\cos(\psi) + V_y\sin(\psi)$
Y	*Global Y axis coordinate*	$\dot{y} = V_x\sin(\psi) + V_y\cos(\psi)$

♣ Simulation results

We tested the dynamic model developed in the previous stage; parameters of this model are described in the following table:

Table II.3: parameters of this model of the four-wheeled mobile robot

symbol	**Name**	**value**
V_x	*The longitudinal velocity at c.g. of vehicle*	$10m/s$
C_f	*The cornering stiffness of the front tire*	$1231N/rad$
C_r	*The cornering stiffness of the rear tire*	$1231N/rad$
l_f	*The longitudinal distance of the front tire*	$0.67m$
l_r	*The longitudinal distance of the rear tire*	$1.1m$
I_z	*The yaw-inertia moment*	$300kg.m^2$

We put the value of the front and rear steering angle of the vehicle at $\delta_f = 0$ and $\delta_r = 0.3$ and we get as simulation results, shown in following:

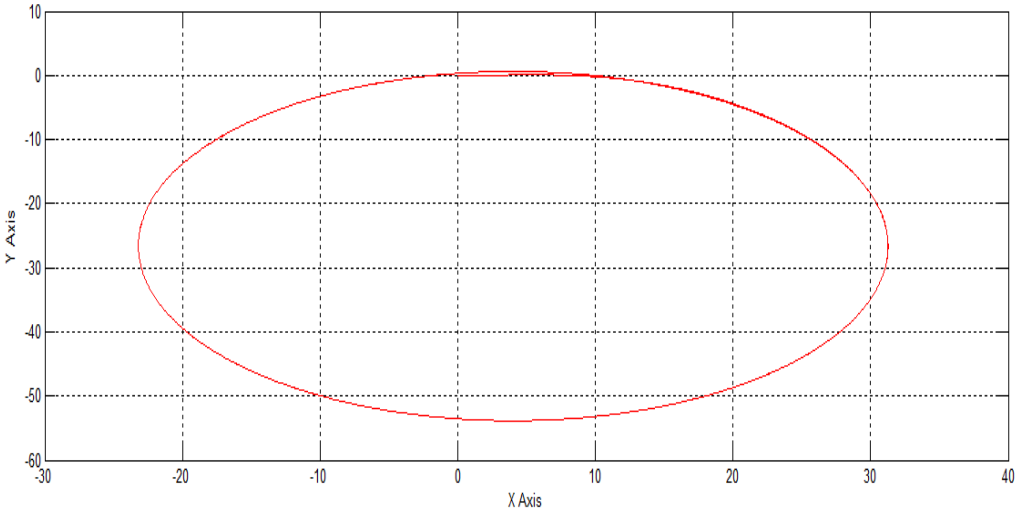

Fig. II.6: Vehicle trajectory for $V_x = 10m/s$

II.6 Conclusion

In this chapter, the kinematic mode of the lateral movement of the vehicle has been developed, and we developed the dynamic behavior of the vehicle in a dynamic model. This model is presented in state space model.

These models have been tested to recognize their validity, and we provide results of those tests in figures.

These models are prepared to be able to handle the control law, where will be highlighted in the next chapter.

Chapter III

Development of The Control Law NCGPC

III.1 Introduction

Predictive control technic is one of the advanced techniques in the science of automation. It has emerged as a solution to many problems in the world of industry, including dealing with complex systems or systems with limitations.

This technique has become a good alternative to classical control techniques (for example PID).

Predictive control is capable to predict the future behavior of a system, which allows the control law to deal smoothly with changes in system behavior.

What increases the power of this technic is the ability to deal with linear and nonlinear systems.

The predictive control law has been produced in several algorithms. In this work, we are interested to use the Non-linear Continuous-time Generalized Predictive Control (NCGPC) as control law with a multi-input multi-output system (MIMO).

In this chapter, we will present a general explanation to control systems, and then explain the principle of predictive control.
The approach adopted in this work (NCGPC) will be presented in detail.

In addition, we will explain how this approach deals with multi-input multi-output systems, and the mathematical tools used to facilitate dealing with these systems.

Calculation of prediction error and the performance rate are required to develop the control law, which will be developed in this chapter.

III.2 Overview of control system

A control system is an interconnection of components forming a system configuration that will provide the desired system response.

The input-output relationship represents the cause-and-effect relationship of the process, which in turn represents a processing of the input signal to provide an output signal variable [Lss01].

Systems can be grouped into two main types, Open loop control systems, and Closed-loop control systems.

An open-loop control system is a kind of system whereby the output has no effect on the actual conditions encountered, which means, no feedback is involved in this particular system.

The open-loop control system is usually unsatisfactory because the system cannot compensate for any disturbance that occurs. Thus, the open-loop control system is not suitable for systems that are difficult to control. The closed-loop control system is also known as feedback control system.This form of the control system has one or more feedback loops or circuits that seek to overcome the errors inherent in the system. This means the output from the system will be measured and compared with the input in order to ensure that the derived output is ascertained even before it is rectified by the controller [SNZ10].

A control unit can be any type of controllers known in automatic science.

Most systems use the PID as a controller in the control loop, which can be defined as:

The Proportional–integral–derivative (PID) controller is the most common form of feedback. It was an essential element of early governors and it became the standard tool when process control emerged in the 1940s. In process control today, more than 95% of the control loops are of PID type, most loops are actually PI control. PID controllers are today found in all areas where control is used [Ås02].

Even though versatile, the PID controller has weaknesses that limit its achievable performance especially on dead-time dominant, inverse response, poorly damped, and non-linear processes [Gio09] [Wan08] [KM01].

Since the system that we are dealing with is a multi-input and output system, and since expecting the future behavior is very important in the case of our system, we will not depend on the PID controller as a controller in the control loop, but will be replaced by a controller based on the predictive control approach, which will be addressed in detail in the next stage.

III.3 Principle of predictive control

The predictive control algorithm takes into account the future behavior of the system in order to develop a control allowing the best follow-up of a known trajectory [BOU11] [CEF04] [R01].

This idea is simple and practiced regularly in everyday life. For example, the driver defines the specific path (the road), the specified control horizon (the driver's visual field), and takes into account the characteristics of the vehicle (the mental model of the behavior of the vehicle), and then decides which actions: (acceleration, brake or steering wheel operation) must apply at that moment. This principle includes several activities in our daily lives, where predictive control is used in activities such as walking, skiing, etc [Ahm15].

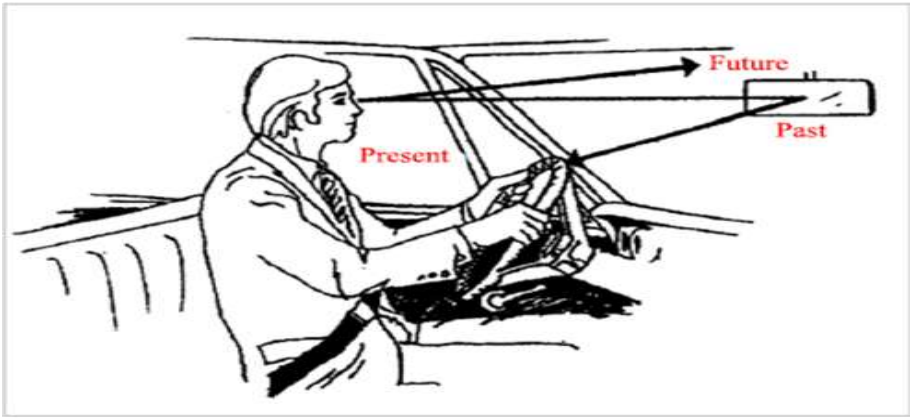

Fig. III.1: Philosophy of Predictive Control

III.3.1 Generalized predictive control (GPC)

Generalized prediction control is one of the predictive control algorithms, where the variables involved are defined in the choice of control over a given time range, this future time horizon with a limited horizon is called prediction horizon.

The principle of predictive control is based on take into account: current time, future behavior, using a numerical model to predict future outputs in a limited horizon.

One of the advantages of predictive methods is:
That in order to reach a point that has already been set in a certain horizon, it is possible to exploit the information of future paths predetermined, because the target is matching the results of the system with this point on the limited horizon [sm09].

III.3.2 Main component of the predictive control

The generalized predictive control is based on four main components:

1. The Prediction: creation of an anticipatory effect by exploiting a trajectory to follow in the future. [Ahm15]

2. Prediction model: a model of the system to predict the future development of outputs on the prediction horizon: $Np:\ \hat{y} = [\hat{y}(k)\,\hat{y}(k+1)\ldots.\hat{y}(k+Np)]$ [Ahm15].

3. Optimization method: to calculate a sequence of commands on the control horizon Nu: $\theta = [u^*(k)\,u^*(k+1)\ldots u^*(k+Nu)]$ which minimizes the optimization criterion J by satisfying the constraints imposed by the user, which $u^*(k+i) = u^*(k+Nu)$ for $Nu \leq i \leq Np$ [Ahm15].

4. Principle of the sliding horizon: This is based on moving the horizon $k \to k+1$ each sampling period after applying the first control $u^*(k)$ of the optimal sequence thus obtained [Ahm15].

The predictive control law is determined by solving the optimal control problem in a limited horizon (as shown in Figure III.1) of the reference path to be followed, which is known in advance. The following steps should be applied in each sampling period:

- ❉ Calculate the prediction of output variables $\hat{y}$ in prediction horizon on the output Np
- ❉ Reduction of the limited horizon criterion based on: future prediction errors, variance between expected system output and future target point.
- ❉ Obtain a series of future commands on the control horizon less or equal Np.
- ❉ Apply only the first value of this sequence to the system.
- ❉ Repeat these steps in each sampling period [Bez13].

These elements are summarized in the following figure(III.2)

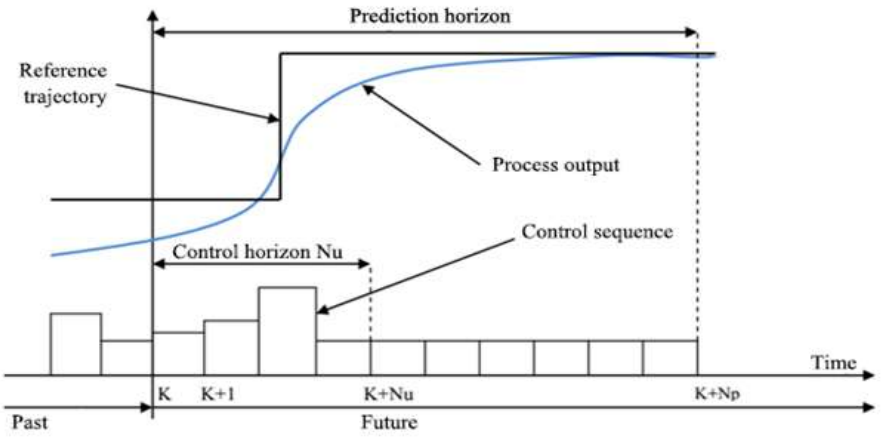

Fig. III.2: Predictive control strategy

Predictive control algorithms are divided into several sections as needed by the user. From the generalized prediction control(GPC) that has been discussed previously, there

is an algorithm for the generalized prediction(GPC) of linear systems and the other for nonlinear systems(GPC), in addition to the predictive control model(MPC) based on a model as the principle of it's function.

The predictive control has been used to control a wide range of processes, those with simple dynamics to more complex mechanisms, for example, late or unstable systems.

The multivariate case is easily handled.

The relatively easy setting of it's parameters makes it accessible to people with limited knowledge in automatic.

The treatment of constraints imposed on the control system can be included in obtaining the control law.

It is very efficient when the instructions or trajectories to follow are known in advance (which is the case in several industrial processes such as digital machines and robots) [Bez13].

We chose the Non-linear Continuous-time Generalized Predictive Control (NCGPC) to match the system we will deal with in this work, since the nature of this system is a multi-input and output system, and as it is a robot, we dealing with it in real time.

III.4 Non-linear Continuous-time Generalized Predictive Control

Predictive control is an optimal command based on the minimization of a quadratic criterion composed of the error between the predicted output and the reference.

The advantage of this method is that it applies to nonlinear systems as they are, hence the term "nonlinear continuous generalized Predictive Control" (NCGPC).

The prediction is based on a Taylor series development and the knowledge of the derivatives of the dynamic function of the system up to the so-called relative degree order.

In this section, we present this technique applied to systems multi-input-multi-output (MIMO). Of course, the method can be applied to single-input single-output systems (SISO), it suffices to reduce the size of the input and the output to one [Kri12].

III.4.1 System multi-input multi-output

A MIMO nonlinear system can be written in the following form:

$$\begin{aligned} \dot{x} &= f(x) + \sum_{i=1}^{p} g(x)u_i \\ y &= (h_1(x) \ldots . h_m(x)) \end{aligned} \tag{III.1}$$

Where, the state vector $x \in X \subset \Re^n$, the output $y \in Y \subset \Re^m$,and the control $u \in U \subset \Re^p$. With X Belongs to $\Re^n$ and U and Y Belongs to $\Re^p$ and $\Re^m$ respectively. Mention that this type of system, as shown (III.1) is nonlinear in the state and refines in the order. This property is essential to use this control law.

The NCGPC technique consists in minimizing a quadratic criterion that is based on the difference between the predicted state and a reference signal. Our goal is to treat an

asymptotic tracking trajectory problem while minimizing a defined cost function [Kri12].

This is related to a fixed reference signal, that we note ω (t) and to make the output $y(t)$ tend towards ω (t) by using an optimal control law on all the horizon of prediction.

So, is $\omega \in \Re^m$ the reference vector such as $\omega = (\omega_1(t) \cdots \omega_m(t))$ and $e \in \Re^m$ the error vector defined by the following expression:

$$e_i = h_i(x(t)) - \omega_i(t) \tag{III.2}$$

With $h_i(x(t))$ the i-th component of the output vector Y.

The variable t is considered as the moment present. We designate by τ the moment at which the prediction will be made and by T^i the prediction horizon onthe error e^i. Therefore, we can write the quadratic criterion for each components $h_i(x(t))$ of the output y in the form:

$$J_i = \frac{1}{2}\int_0^{T_i} [\hat{e}_i(t+\tau)]^2 d\tau \tag{III.3}$$

Hence the global criterion J such that:

$$J = \sum_{i=1}^{m} j_i = \frac{1}{2}\sum_{i=1}^{m}\left(\int_0^{T_i} [\hat{e}_i(t+\tau)]^2 d\tau\right) \tag{III.4}$$

So, the objective of the order will be the minimization of the global criterion Jm To express the predicted error, we need some notions about Lie derivatives of nonlinear functions. Next, the prediction of the output and of the reference trajectory will be detailed to be able to write the criterion to be minimized and finally to deduce the control law [Kri12].

III.4.2 Lie derivatives

To simplify the presentation in the remainder of the memory, we use the standard notation of Lie derivatives and we keep the same parameters of the system. The Lie derivative of the output h_i along f in $x \in \Re^n$, denoted by $L_f h_i(x)$, is given by the following expression:

$$L_f h_i(x) = \sum_{j=1}^{n} \frac{\partial h_i}{\partial x_i}(x) f_i(x) \tag{III.5}$$

Inductively, we define

$$L_f^k h_i(x) = L_f L_f^{k-1} h_i(x) = \frac{\partial L_f^{k-1} h}{\partial x}(x) f(x) \tag{III.6}$$

with $L_f^0 h_i(x) = h_i(x)$

We define by ρ the relative degrees vector composed by the relative degrees ρ_i specific to each of the h_i outputs. The relative degree of an output is the minimum number of

derivations of this output necessary to make appear explicitly in its expression at least one component of the input vector. A non-linear MIMO system, of the form (III.1) , has a relative degree vector

$\rho = (\rho_1(t) \cdots \rho_m(t))$ around x^0 if:

1. $L_{g_i} L_f^k h_i(x) = 0$ for all $1 \leq j \leq p$ for all $k \prec \rho_i - 1$, for all $1 \leq i \leq m$ and all x in a neighborhood of x^0

2. the matrix D(x) of dimension $m \times m$,called the decoupling matrix, given by:

$$D(x) = \begin{pmatrix} L_{g_1} L_f^{\rho_1 - 1} h_1(x) & \dots & L_{g_p} L_f^{\rho_1 - 1} h_1(x) \\ \vdots & \ddots & \vdots \\ L_{g_1} L_f^{\rho_m - 1} h_m(x) & \cdots & L_{g_p} L_f^{\rho_m - 1} h_m(x) \end{pmatrix} \tag{III.7}$$

is not singular in $x = x^0$

As said previously, the relative degree is the order of the derivative from which the control term appears. Since this term is linear and given the affine structure of the control terms in the state equation, it is therefore easy to predict the output to a certain time horizon, to formulate the optimization problem, in a form quadratic and finally to extract the solution in an analytical form [Kri12].

III.4.3 Error prediction

The prediction of the output is deduced from it's Taylor series development. Taylor's serial development of the output y at the instant $(t+\tau)$, up to an order, equal to the relative degree ρ, is given by:

$$\hat{y}(t+\tau) = \sum_{k=0}^{\rho} y^{(k)}(t) \frac{\tau^k}{k!} + R(\tau^\rho) \tag{III.8}$$

Where t corresponds to the present instant and $(t+\tau)$ to the prediction instant. The term $R(\tau^\rho)$ represents the higher order elements of development which, when neglected, give the following equation:

$$\hat{y}(t+\tau) \approx \sum_{k=0}^{\rho} y^{(k)}(t) \frac{\tau^k}{k!} \tag{III.9}$$

The predicted output is written in the following matrix form:

$$\hat{y}(t+\tau) \cong \begin{bmatrix} 1 & \tau & \frac{\tau^2}{2!} \cdots & \frac{\tau^\rho}{\rho!} \end{bmatrix} \begin{bmatrix} y(t) \\ \dot{y}(t) \\ \vdots \\ y^{(\rho-1)}(t) \\ y^\rho(t) \end{bmatrix} \tag{III.10}$$

whose output $y(t)$ and it's derivatives up to the order τ are given by:

$$\left\{\begin{array}{c} y(t)=h(x(t)) \\ \dot{y}(t)=L_f h(x(t)) \\ \vdots \\ y^{(\rho-1)}(t)=L_f^{\rho-1}h(x(t)) \\ y^{\rho}(t)=L_f^{\rho}h(x(t))+L_g L_f^{\rho-1}h(x(t))u(t) \end{array}\right\} \tag{III.11}$$

Therefore, the prediction of the output is:

$$\hat{y}(t+\tau)\cong\begin{bmatrix}1 & \tau & \frac{\tau^2}{2!}\cdots & \frac{\tau^{\rho}}{\rho!}\end{bmatrix}\begin{bmatrix} h(x(t)) \\ L_f h(x(t)) \\ \vdots \\ L_f^{\rho-1}h(x(t)) \\ L_f^{\rho}h(x(t))+L_g L_f^{\rho-1}h(x(t))u(t)\end{bmatrix} \tag{III.12}$$

Similarly, assuming that the reference signal $\omega(t)$ is known and ρ derivable, the expression of its estimate $\hat{\omega}$ can be deduced at the instant $(t+\tau)$ in a form similar to that of the output (t), from where

$$\hat{\omega}(t+\tau)\cong\begin{bmatrix}1 & \tau & \frac{\tau^2}{2!}\cdots & \frac{\tau^{\rho}}{\rho!}\end{bmatrix}\begin{bmatrix} \omega(t) \\ \dot{\omega}(t) \\ \vdots \\ \omega^{(\rho-1)}(t) \\ \omega^{(\rho)}(t)\end{bmatrix} \tag{III.13}$$

Thus, it is possible to define the prediction error predicted at the instant $(t+\tau)$ As follows:

$$\hat{e}_i(t+\tau)=\hat{y}_i(t+\tau)-\hat{\omega}_i(t+\tau) \tag{III.14}$$

with $1\leq i\leq m$ and $\hat{e}_i$ the error of prediction of the i-th output of the system.

The prediction error in it's matrix form becomes:

$$\hat{e}_i(t+\tau)\cong\begin{bmatrix}1 & \tau & \frac{\tau^2}{2!}\cdots & \frac{\tau^{\rho_i}}{\rho_i!}\end{bmatrix}\begin{bmatrix} e_i(t) \\ \dot{e}_i(t) \\ \vdots \\ e^{(\rho_i-1)}(t) \\ e^{(\rho_i)}(t)\end{bmatrix} \tag{III.15}$$

by posing:

$$E_i(t) = \begin{bmatrix} e_i(t) \\ \dot{e}_i(t) \\ \vdots \\ e^{(\rho_i-1)}(t) \\ e^{(\rho_i)}(t) \end{bmatrix} and \Lambda_i(\tau) = \begin{bmatrix} 1 \\ \tau \\ \vdots \\ \frac{\tau^{\rho_i-1}}{\rho_i-1!} \\ \frac{\tau^{\rho_i}}{\rho_i!} \end{bmatrix}^t \tag{III.16}$$

the predicted error becomes:

$$\hat{e}_i(t+\tau) = \Lambda_i(\tau)E_i(t) \tag{III.17}$$

In the next paragraph, we then take up the quadratic criterion in its matrix form for the development of the control law.

III.4.4 Quadratic criterion

The criterion we will consider here is the sum of all the criteria quadratic, constructed on each of the outputs of the system. We can rewrite the criterion J defined in (III.4) in the following matrix form:

$$J_i(t) = \frac{1}{2}\int_0^{T_i} E_i^t(t)\Lambda_i^t(\tau)\Lambda_i(\tau)E_i(t)d\tau \tag{III.18}$$

Since the vector E_i does not depend on the variable τ but on the variable t, then

$$J_i(t) = \frac{1}{2}E_i^t(t)\int_0^{T_i} \Lambda_i^t(\tau,\rho_i)\Lambda_i(\tau,\rho_i)d\tau E_i(t) \tag{III.19}$$

For practical reasons of condensation, put the matrix $\Pi_i(T_i,p_i)$ of dimensions $(\tau+1)\times(\tau+1)$, one defines then the "matrix of prediction" as follows

$$\prod_i(T_i,\rho_i) = \int_0^{T_i} \Lambda_i^t(\tau,\rho_i)\Lambda_i(\tau,\rho_i)d\tau \tag{III.20}$$

The criterion J_i can be written as follows:

$$J_i(t) = \frac{1}{2}E_i^t(t)\prod_i(T_i,\rho_i)E_i(t) \tag{III.21}$$

We then deduce the global criterion J in its matrix form:

$$J(t) = \frac{1}{2}E^t(t)\prod(T,\rho)E(t) \tag{III.22}$$

III.4.5 Development of the control law

The NCGPC control law is developed for the purpose of asymptotic tracking of a reference signal while minimizing the quadratic criterion built on the prediction error

(III.22). However, this operation requires verification of the following A1 to A4 assumptions [Kri12]:

A1: the dynamics of zeros exists and is asymptotically stable.

A2: all states are measurable.

A3: the system studied has a relative vector degree ρ well defined.

A4: the components of the output $y(t)$ and of the reference signal $\omega(t)$ are sufficiently several times continuously differentiable with respect to time.

The control law is elaborated starting from the minimization of the criterion (III.18) with respect to the control U, from where:

$$\frac{\partial J}{\partial u} = 0_{p\times 1} \tag{III.23}$$

In a more detailed way, this is written:

$$\frac{\partial J}{\partial u} = \frac{1}{2}\sum_{i=1}^{m} \frac{\partial \left[E_i^t(t)\prod_i(T_i,\rho_i)E_i(t)\right]}{\partial u} = 0_{p\times 1} \tag{III.24}$$

To make the command appear in the expression of the quadratic criterion above we use the expression of the error vector E_i

$$E_i(t) = \begin{bmatrix} h_i(x(t)) - \omega_i(t) \\ L_f h_i(x(t)) - \dot{\omega}_i(t) \\ \vdots \\ L_f^{(\rho_i-1)} h_i(x(t)) - \omega_i^{(\rho_i-1)}(t) \\ L_f^{(\rho_i)} h_i(x(t)) - \omega_i^{(\rho_i)}(t) + u L_g L_f^{(\rho_i-1)} h_i \end{bmatrix} \tag{III.25}$$

$$E_i(t) = \begin{bmatrix} h_i(x(t)) - \omega_i(t) \\ L_f h_i(x(t)) - \dot{\omega}_i(t) \\ \vdots \\ L_f^{(\rho_i-1)} h_i(x(t)) - \omega_i^{(\rho_i-1)}(t) \\ L_f^{(\rho_i)} h_i(x(t)) - \omega_i^{(\rho_i)}(t) + \begin{bmatrix} L_{g_1} L_f^{(\rho_i-1)} h_i & \cdots & L_{g^\rho} L_f^{(\rho_i-1)} h_i \end{bmatrix} \begin{bmatrix} u_1 \\ \vdots \\ u_\rho \end{bmatrix} \end{bmatrix} \tag{III.26}$$

The equation (III.24) then becomes:

$$\frac{\partial J}{\partial u} = \frac{1}{2}\sum_{i=1}^{m} \left(\frac{\partial E_i(t)}{\partial u}\right)^t \prod_i (T_i,\rho_i) E_i(t) = 0_{p\times 1} \tag{III.27}$$

Or again

$$\frac{\partial J}{\partial u} = \frac{1}{2}\sum_{i=1}^{m} \begin{bmatrix} 0_{\rho_i \times 1} & \cdots & 0_{\rho_i \times 1} \\ L_{g_1} L_f^{(\rho_i - 1)} h_i & \cdots & L_{g^\rho} L_f^{(\rho_i - 1)} h_i \end{bmatrix}^t \prod_i (T_i, \rho_i) E_i(t) = 0_{p \times 1} \tag{III.28}$$

To simplify the expression, we define Π_i^s the last line of the matrix Π_i. Thus, it is possible to put the derivative of the criterion J_m with respect to the elements of the control vector u in the form:

$$\frac{\partial J}{\partial u} = \frac{1}{2}\sum_{i=1}^{m} \begin{bmatrix} L_{g_1} L_f^{(\rho_i - 1)} h_i \\ \vdots \\ L_{g^\rho} L_f^{(\rho_i - 1)} h_i \end{bmatrix}_{(p \times 1)} \prod_i^s (T_i, \rho_i) E_i(t) = 0_{p \times 1} \tag{III.29}$$

When we expand the sum of the equation above, we get:

$$\begin{bmatrix} L_{g_1} L_f^{(\rho_1 - 1)} h_1 \\ \vdots \\ L_{g^\rho} L_f^{(\rho_1 - 1)} h_1 \end{bmatrix} \prod_1^s (T_1, \rho_1) E_1(t) + \cdots + \begin{bmatrix} L_{g_1} L_f^{(\rho_m - 1)} h_m \\ \vdots \\ L_{g^\rho} L_f^{(\rho_m - 1)} h_m \end{bmatrix} \prod_m^s (T_m, \rho_m) E_m(t) = 0_{p \times 1} \tag{III.30}$$

We can put this equation in the form:

$$\begin{bmatrix} L_{g_1} L_f^{(\rho_1 - 1)} h_1 & \cdots & L_{g_1} L_f^{(\rho_m - 1)} h_m \\ \vdots & \ddots & \vdots \\ L_{g^\rho} L_f^{(\rho_1 - 1)} h_1 & \cdots & L_{g^\rho} L_f^{(\rho_m - 1)} h_m \end{bmatrix}_{(p \times m)} \begin{bmatrix} \prod_1^s E_1 \\ \vdots \\ \prod_m^s E_m \end{bmatrix}_{(m \times 1)} = 0_{p \times 1} \tag{III.31}$$

The first term of the equation represents the transpose of the decoupling matrix $D(x)$. We can therefore deduce that the second term of the equation is zero because $D(x)$ is nonzero by construction. We can therefore deduce that:

$$\begin{bmatrix} \prod_1^s E_1 \\ \vdots \\ \prod_m^s E_m \end{bmatrix}_{(m \times 1)} = 0_{m \times 1} \tag{III.32}$$

If we take, again the expression of E_i presented in (III.26), one deduces that the equation (III.32) depends on the command u. The two equations (III.26) and (III.32) are combined and rewritten as (III.33). From this equation, the entry u in (III.34) appears with Π_i^{ss} corresponding to the last term of the vector Π_i^s previously defined. It is recalled that the decoupling matrix $D(x)$ is non-zero. However, it must be emphasized that it is not necessarily square because of $p \leq m$. To determine the command, we must then calculate the inverse of the matrix $D^t(x)D(x)$. For this we suppose that det $(D^t(x)D(x))$ is nonzero. This condition will be taken into account when implementing the command, and so to cancel the command if the condition is not fulfilled (i.e. if $det(D^t(x)D(x)) = 0$). Finally, we deduce our command law from (III.35) with $k_{i=}\prod_i^s / \prod_i^{ss}$. [Kri12]

Where K_i is the gain matrix and it can be calculated in general form by the following steps [Dab10]:

$K = K(T,\rho)$, which $K = \prod_{ss}^{-1} \prod_s$

We suppose

$K(T,\rho) = \Pi_{ss}^{-1}(T,\rho)\Pi_s(T,\rho)$, and $L = j-1$

It becomes

$K_{\rho l}(T,\rho) = \frac{\rho!}{L!T^{\rho-L}} \frac{(2\rho+1)}{(\rho+L+1)}$

For all $0 \leq L = j-1 \leq \rho$. In the case where $j = \rho+1$ (or $L = \rho$)

$K_{\rho\rho}(T,\rho) = \frac{\rho!(2\rho+1)}{\rho!(2\rho+1)T^0} = 1$

We rewrite $K(T,\rho)$ in matrix form, it becomes:

$$K(T,\rho) = \left[\frac{\rho!}{T^\rho}\frac{2\rho+1}{\rho+1} \quad \cdots \quad \frac{\rho!}{T^{\rho-L}}\frac{2\rho+1}{(L)!(\rho+L+1)} \quad \cdots \quad 1\right]$$

$$
\begin{bmatrix} \Pi_1^s E_1 \\ \vdots \\ \Pi_m^s E_m \end{bmatrix}_{(m\times 1)} = \begin{bmatrix} \Pi_1^s & & 0 \\ & \ddots & \\ 0 & & \Pi_m^s \end{bmatrix} \begin{bmatrix} h_1 - \omega_1 & & & 0 & & \\ L_f h_1 - \dot{\omega}_1 & & & \vdots & & \\ \vdots & + & & & & \\ L_f^{\rho_1 - 1} h_1 - \omega_1^{(\rho_1 - 1)} & & \begin{bmatrix} L_{g1} L_f^{(\rho_i - 1)} h_1 & \dots & L_{g_p} L_f^{(\rho_i - 1)} h_1 \end{bmatrix} & & \begin{bmatrix} u_1 \\ \vdots \\ u_p \end{bmatrix} \\ L_f^{\rho_1} h_1 - \omega_1^{(\rho_1)} & & & & & \\ \vdots & \vdots & & \vdots & & \\ h_m - \omega_m & & & 0 & & \\ L_f h_m - \dot{\omega}_m & & & \vdots & & \\ \vdots & + & & & & \\ L_f^{\rho_1 - 1} h_m - \omega_m^{(\rho_m - 1)} & & \begin{bmatrix} L_{g1} L_f^{(\rho_i - 1)} h_m & \dots & L_{g_p} L_f^{(\rho_i - 1)} h_m \end{bmatrix} & & \begin{bmatrix} u_1 \\ \vdots \\ u_p \end{bmatrix} \\ L_f^{\rho_m} h_m - \omega_m^{(\rho_m)} & & & & & \end{bmatrix} \tag{III.33}
$$

$$\begin{bmatrix} \Pi_1^{ss} & & 0 \\ & \ddots & \\ 0 & & \Pi_m^{ss} \end{bmatrix} \begin{bmatrix} L_{g1}L_f^{(\rho_1-1)}h_1 & \cdots & L_{g_p}L_f^{(\rho_1-1)}h_1 \\ \vdots & \ddots & \vdots \\ L_{g1}L_f^{(\rho_m-1)}h_m & \cdots & L_{g_p}L_f^{(\rho_m-1)}h_m \end{bmatrix} \begin{bmatrix} u_1 \\ \vdots \\ u_p \end{bmatrix} = - \begin{bmatrix} \Pi_1^{s} & & 0 \\ & \ddots & \\ 0 & & \Pi_m^{s} \end{bmatrix} \begin{bmatrix} h_1 - \omega_1 \\ \vdots \\ L_f^{\rho_1}h_1 - \omega_1^{(\rho_1)} \\ \vdots \\ h_m - \omega_m \\ \vdots \\ L_f^{\rho_m}h_m - \omega_m^{(\rho_m)} \end{bmatrix} \tag{III.34}$$

$$\begin{bmatrix} u_1 \\ \vdots \\ u_p \end{bmatrix} = -\Big(D^t(x)\,D(x)\Big)^{-1}\; D^t(x) \quad \underset{\left[p\times\sum_{i=1}^{m}(\rho_i+1)\right]}{\begin{bmatrix} k_1 & & 0 \\ & \ddots & \\ 0 & & k_m \end{bmatrix}} \quad \underset{\left[\sum_{i=1}^{m}(\rho_i+1)\times 1\right]}{\begin{bmatrix} h_1 - \omega_1 \\ \vdots \\ L_f^{\rho_1}h_1 - \omega_1^{(\rho_1)} \\ \vdots \\ h_m - \omega_m \\ \vdots \\ L_f^{\rho_m}h_m - \omega_m^{(\rho_m)} \end{bmatrix}} \tag{III.35}$$

Finally, we can write the expression of the command U as follows:

$$U = -(D^t(x)D(x))^{-1}D^t(x)KE_p \tag{III.36}$$

With $D(x)$ the decoupling matrix. The gain matrix K and the matrix of the predicted error E_p are as follows:

$$K = \begin{bmatrix} \prod_1^{ss} & & 0 \\ & \ddots & \\ 0 & & \prod_m^{ss} \end{bmatrix}^{-1} \begin{bmatrix} \prod_1^{s} & & 0 \\ & \ddots & \\ 0 & & \prod_m^{s} \end{bmatrix} \tag{III.37}$$

$$E_p = \begin{bmatrix} h_1 - \omega_1 \\ \vdots \\ L_f^{\rho_1} h_1 - \omega_1^{(\rho_1)} \\ \vdots \\ h_m - \omega_m \\ \vdots \\ L_f^{\rho_m} h_m - \omega_m^{(\rho_m)} \end{bmatrix} \tag{III.38}$$

III.5 Conclusion

The goal of this chapter is preparing the control law after a mathematical development of the prediction model, which allows the system to track a given trajectory and get the best possible results of the trajectory tracking, depending on minimizing the error between the target and the output.

The control law has been developed in the case of a multi-input and multi-output system (MIMO), where, we addressed the way that this law was treated the multi-input and multi-output systems, as well as the necessary elements for the development of the control law, such as calculation of prediction error and performance rate.

As a result, the application of the Nonlinear Continuous-time Generalized Predictive Control (NCGPC) approach is very useful for the state of the system that we handle. Synthesis of the control and the trajectory tracking results will be addressed in the next chapter.

Chapter IV

Simulation results and discussion

IV.1 Introduction

The theoretical aspect allows us to understand the reality of things, but the practical side highlights the characteristics and importance of these things. Therefore, we have to try the control law developed in the previous stage, to show up the importance and advantages of this approach, and after that, we can judge it.

In this chapter we will present an example of an application in order to study the performance of nonlinear continuous-time generalized predictive control (NCGPC) approach, it's applied in a vehicle-type mobile robot.

The control law will be synthesized prior to the experiment and will be applied to the mathematical model of the vehicle in stages.

Initially, a small speed will be chosen for the vehicle with various prediction horizons, and then to a relatively high speed, and at last to a very high speed. The error is calculated between system outputs(x, y, ψ) and target, where will be displayed in curves. In addition, the results of testing the performance of the control law to track a given path in difficult circumstances will be within this chapter, all these tests will be conducted in order to obtain an overview of the behavior of our system.

The objective from those tests is to know the capability of control law to make the robot track a reference path in various values of the velocity and prediction horizons, and that is through analyzing the results that will be presented in this chapter.

IV.2 Synthesis of the control law

Modeling of the system in the dynamic model was to determine the location of the vehicle, the system outputs are the yaw angle (ψ) and position coordinates (X,Y), and the system inputs are The front steering angle δ_f and The rear steering angle δ_r .

Since we know coordinates of the reference path previously, we can calculate the outputs (ψ,X, Y), and in order to simplify writing of the control law, we have to pass through the Lie derivative, to make that clear we keep the same notation that used before.

We start by the function h_i , which defined the outputs of the system.

$$\begin{Bmatrix} h_1 = \psi \\ h_2 = X \\ h_3 = Y \end{Bmatrix} \tag{IV.1}$$

The vector W. denotes the reference trajectory.

$$W = \begin{pmatrix} w1 \\ w2 \\ w3 \end{pmatrix} = \begin{pmatrix} \psi ref \\ Xref \\ Yref \end{pmatrix} \tag{IV.2}$$

Calculate the vector of relative degree ρ_i is required in the syntheses of the control law, and to get this vector we must use the Lie derivative on the three outputs (ψ,X,Y).

$$\begin{Bmatrix} L_f h_1 = V_\psi \\ L_f h_2 = V_x \cos\psi - V_y \sin\psi \\ L_f h_3 = V_x \sin\psi + V_y \cos\psi \end{Bmatrix} \tag{IV.3}$$

We can notice that $\rho_i > 1$, because for all $i = 1,2,3, L_g L_i = 0$, thus we apply a second time Lie derivative.

$$\begin{Bmatrix} L_f^2 h_1 = \frac{\partial L_f h_1}{\partial V_\psi} f_2 \\ L_f^2 h_2 = \frac{\partial L_f h_2}{\partial V_y} f_1 + \frac{\partial L_f h_2}{\partial V_\psi} f_3 \\ L_f^2 h_3 = \frac{\partial L_f h_3}{\partial V_y} f_1 + \frac{\partial L_f h_3}{\partial V_\psi} f_3 \end{Bmatrix} \tag{IV.4}$$

$$\begin{Bmatrix} L_f^2 h_1 = a_{21} V_y + a_{22} V\psi \\ L_f^2 h_2 = -\sin\psi (V_x V_\psi + a_{11} V_y + a_{12} V_\psi) - V_y V_\psi \cos\psi \\ L_f^2 h_3 = \cos\psi (V_x V_\psi + a_{11} V_y + a_{12} V_\psi) - V_y V_\psi \sin\psi \end{Bmatrix} \tag{IV.5}$$

We notice that the expressions of the $L_{g_j}L_f h_i$ are non-null for all $i=1,2,3$ and $g=1,2$ thus, we can deduce that all terms of the relative degree vector ρ are equal to 2:$\rho=(\rho_1 \quad \rho_2)$

$$\left\{\begin{array}{c} L_{g_1}L_f h_1 = b_{21} \\ L_{g_1}L_f h_2 = -b_{11}\sin\psi \\ L_{g_1}L_f h_3 = b_{11}\cos\psi \end{array}\right\} \tag{IV.6}$$

and

$$\left\{\begin{array}{c} L_{g_2}L_f h_1 = b_{22} \\ L_{g_2}L_f h_2 = -b_{12}\sin\psi \\ L_{g_2}L_f h_3 = b_{12}\cos\psi \end{array}\right\} \tag{IV.7}$$

Finally, the decoupling matrix $D(x)$ can be written as follows.

$$D(x) = \begin{bmatrix} b_{21} & b_{22} \\ -b_{11}\sin\psi & -b_{12}\sin\psi \\ b_{11}\cos\psi & b_{12}\cos\psi \end{bmatrix} \tag{IV.8}$$

From the expression of the control law, we have to verify that the matrix $(D^t(x)D(x))$ is invertible.

The prediction error matrix can be calculating from this expression:

$$Ep = \begin{bmatrix} h_1-\omega_1 \\ L_f h_1-\dot{\omega}_1 \\ L_f^2 h_1-\ddot{\omega}_1 \\ h_2-\omega_2 \\ L_f h_2-\dot{\omega}_2 \\ L_f^2 h_2-\ddot{\omega}_2 \\ h_3-\omega_3 \\ L_f h_3-\dot{\omega}_3 \\ L_f^2 h_3-\ddot{\omega}_3 \end{bmatrix} = \begin{bmatrix} \psi-\omega_1 \\ V_\psi-\dot{\omega}_1 \\ a_{21}V_y+a_{22}V_\psi-\ddot{\omega}_1 \\ X-\omega_2 \\ V_x\cos\psi-V_y\sin\psi-\dot{\omega}_2 \\ -\sin\psi(V_xV_\psi+a_{11}V_y+a_{12}V_\psi)-V_yV_\psi\cos\psi-\ddot{\omega}_2 \\ Y-\omega_3 \\ V_x\sin\psi+V_y\cos\psi-\dot{\omega}_3 \\ \cos\psi(V_xV_\psi+a_{11}V_y+a_{12}V_\psi)-V_yV_\psi\sin\psi-\ddot{\omega}_3 \end{bmatrix} \tag{IV.9}$$

The gain matrix k_i can be calculated from the prediction error k_i :

$$K_i = \begin{bmatrix} \frac{10}{3T_s^2} & \frac{10}{4T_s} & 1 \end{bmatrix} \tag{IV.10}$$

Where T_s is the prediction horizon.

Therefore, we can deduce that the gain matrix write by the following expression:

$$K = \begin{bmatrix} K_1 & 0 & 0 \\ 0 & K_2 & 0 \\ 0 & 0 & K_3 \end{bmatrix} \tag{IV.11}$$

In the end and from what we have previously we can write the control law in its final form (III.36) : $U = -(D^t(x)D(x))^{-1}D^t(x)KE_p$

IV.3 Simulation results

We have reached the most important part of this work, namely the application of the control law on previously studied vehicle model, and the analysis of the obtained results.

These results are the coordinates of the vehicle in a plane(X, Y).

The given path or the reference path will be compared with the path that the vehicle will acquire (the path obtained from the simulation), through change in speed and change of prediction horizon, for the purpose of studying all possible situations and trying to reach the best possible control.

Through the observed results we can judge the ability of Non-linear Continuous-time Generalized Predictive Control approach to track a given path.

We test our system with many different values of the velocity and prediction horizon.

♣ The velocity of the vehicle Vx=10m/s:

✓ Firstly, we set the velocity at 10m/s, and we take different values of prediction horizon $T = 1s, T = 0.7s, T = 0.5s, T = 0.3s$ and we get:

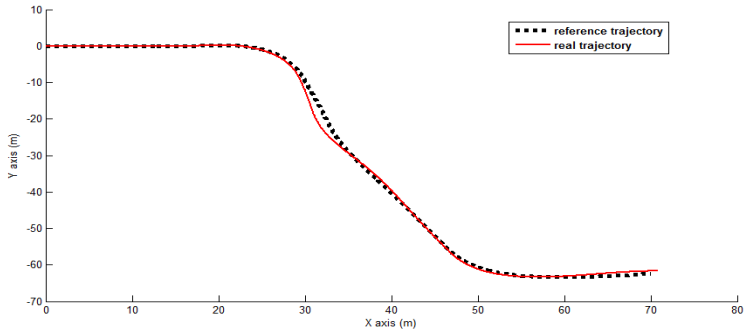

Fig. IV.1: The reference trajectory and the real trajectory at $Vx = 10m/s$ and the prediction horizon at $T = 1s$

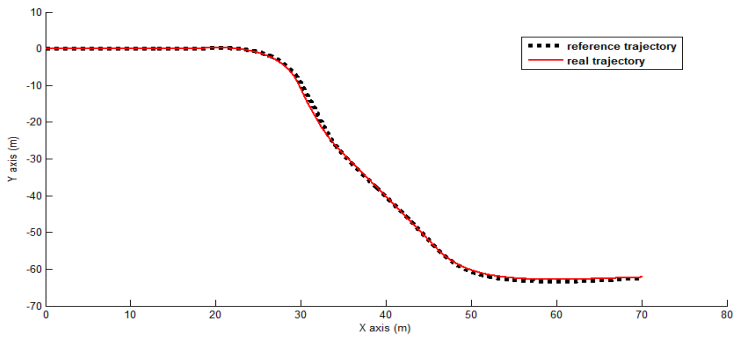

Fig. IV.2: The reference trajectory and the real trajectory at $Vx = 10m/s$ and the prediction horizon at $T = 0.7s$

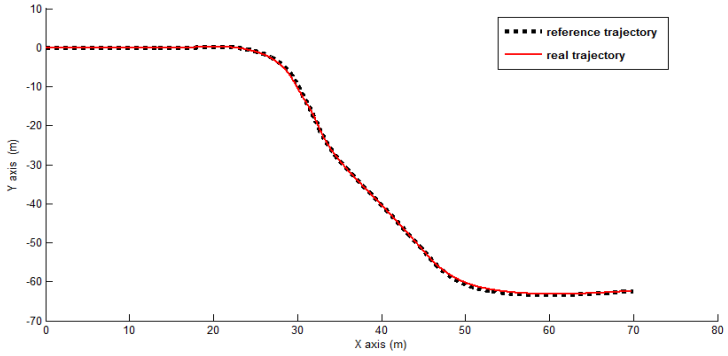

Fig. IV.3: The reference trajectory and the real trajectory at $Vx = 10m/s$ and the prediction horizon at $T = 0.5s$

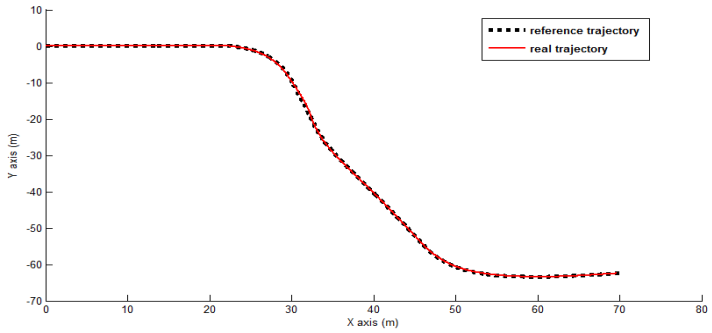

Fig. IV.4: The reference trajectory and the real trajectory at $Vx = 10m/s$ and the prediction horizon at $T = 0.3s$

✠ The error between system inputs and output values (the yaw angle ψ, the position X and Y) at velocity $Vx = 10m/s$ is shown in the following figures respectively:

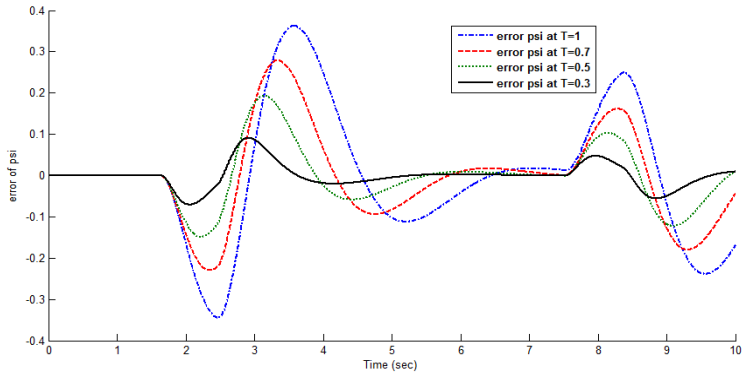

Fig. IV.5: The error between the reference yaw angle ψ and the real yaw angle at $Vx = 10m/s$

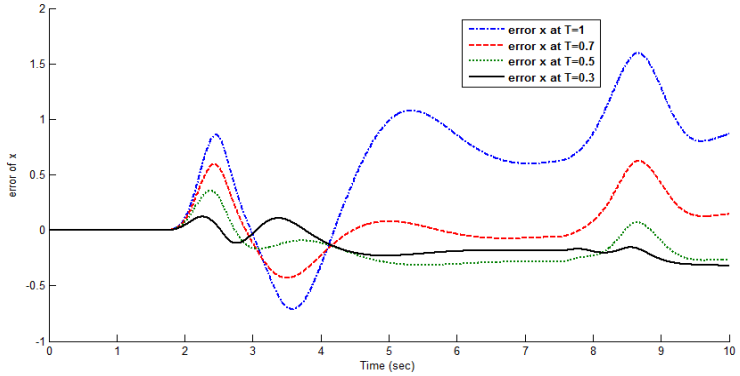

Fig. IV.6: The error between the reference position X and the real position X at velocity $Vx = 10m/s$

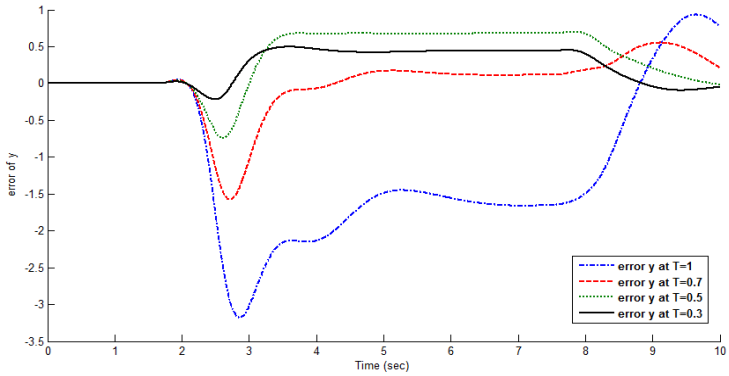

Fig. IV.7: The error between the reference position Y and the real position Y at velocity $Vx = 10m/s$

• The following figures present the control applied to the system inputs (the front and rear steering angles δ_f and δ_r) in different prediction horizons.

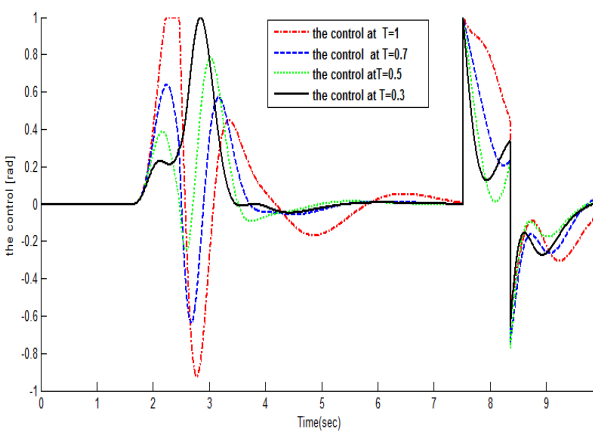

Fig. IV.8: The control applied on the fw

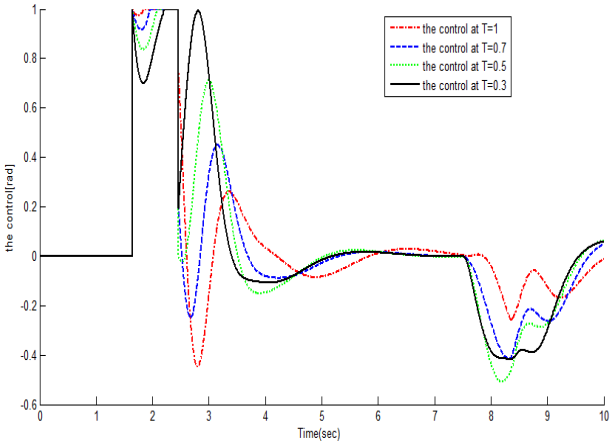

Fig. IV.9: The control applied on the rw

♣ **The velocity of the vehicle Vx=30m/s:**

✓ Secondly, we set the velocity at 30m/s, and we take different values of prediction horizon $T = 0.7s, T = 0.5s, T = 0.3sT = 0.1s$, and we get:

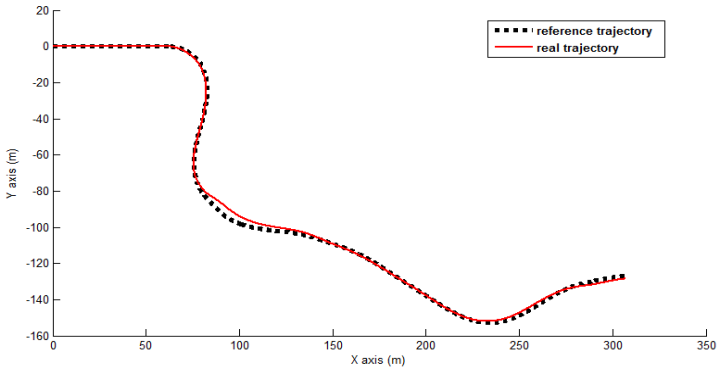

Fig. IV.10: The reference trajectory and the real trajectory at $Vx = 30m/s$ and the prediction horizon at $T = 0.7s$

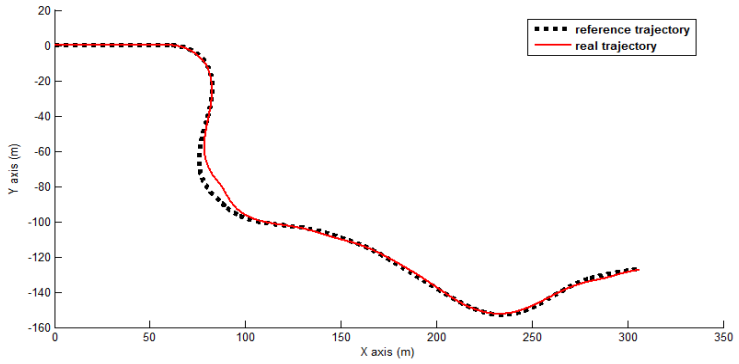

Fig. IV.11: The reference trajectory and the real trajectory at $Vx = 30m/s$ and the prediction horizon at $T = 0.5s$

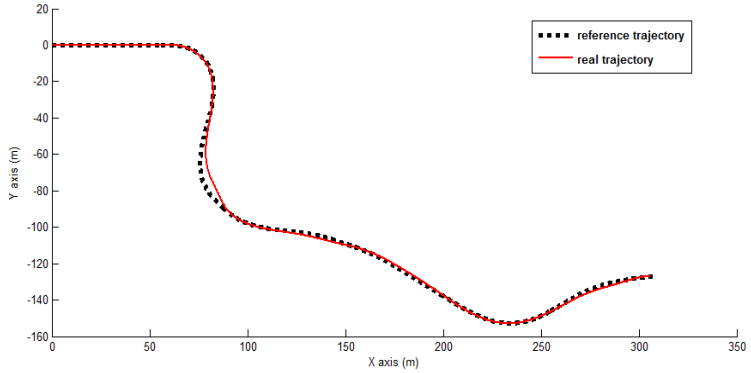

Fig. IV.12: The reference trajectory and the real trajectory at $Vx = 30m/s$ and the prediction horizon at $T = 0.3s$

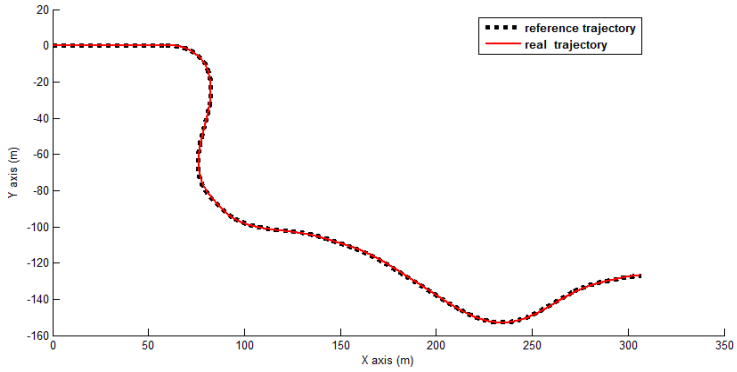

Fig. IV.13: The reference trajectory and the real trajectory at $Vx = 30m/s$ and the prediction horizon at $T = 0.1s$

✠ The error between system inputs and output values (the yaw angle ψ, the position X and Y) at velocity $Vx = 30m/s$ is shown in the following figures respectively:

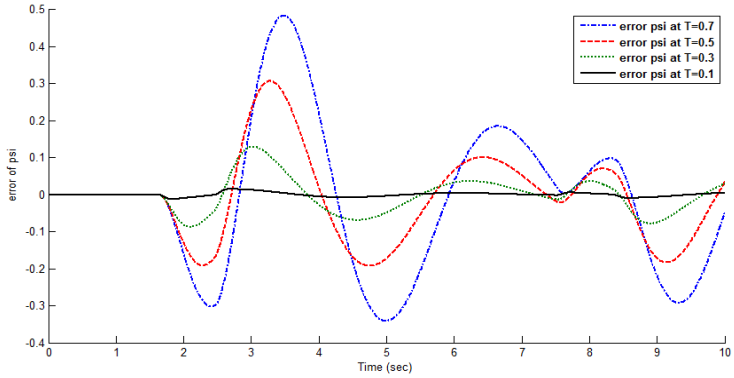

Fig. IV.14: The error between the reference yaw angle ψ and the real yaw angle at $Vx = 30m/s$

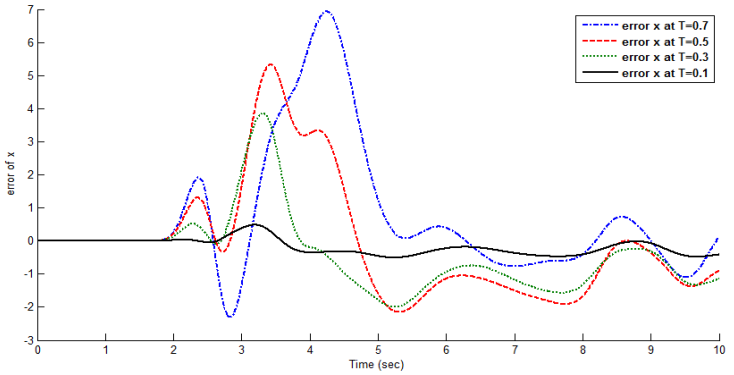

Fig. IV.15: The error between the reference position X and the real position X at velocity $Vx = 30m/s$

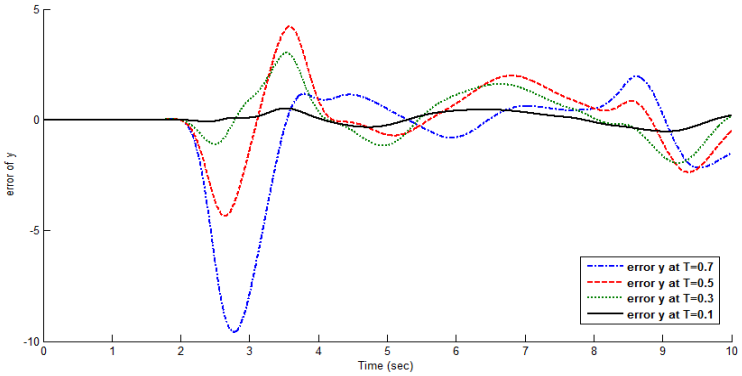

Fig. IV.16: The error between the reference position Y and the real position Y at velocity $Vx = 30m/s$

• The following figures present the control applied to the system inputs (the front and rear steering angles δ_f and δ_r) in different prediction horizons.

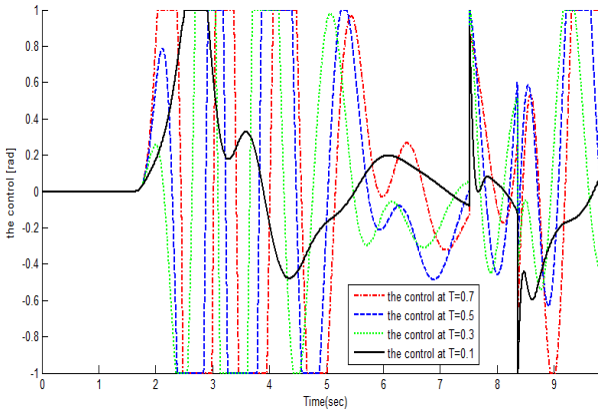

Fig. IV.17: The control applied on the fw

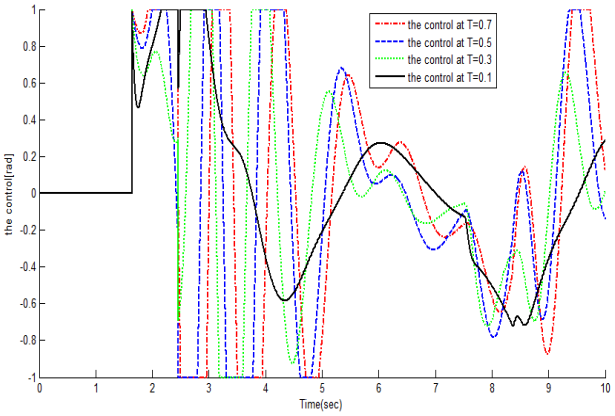

Fig. IV.18: The control applied on the rw

♣ The velocity of the vehicle Vx=50m/s:

✓ Finally, we set the velocity at 50 m/s, and we take different values of prediction horizon $T = 0.5s, T = 0.3s, T = 0.1s, T = 0.07s$, and we get:

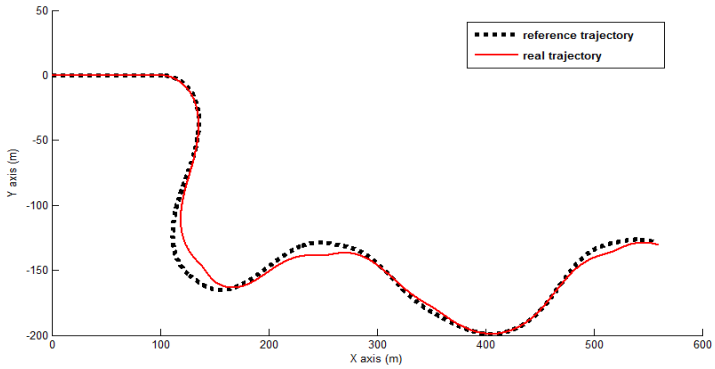

Fig. IV.19: The reference trajectory and the real trajectory at $Vx = 50m/s$ and the prediction horizon at $T = 0.5s$

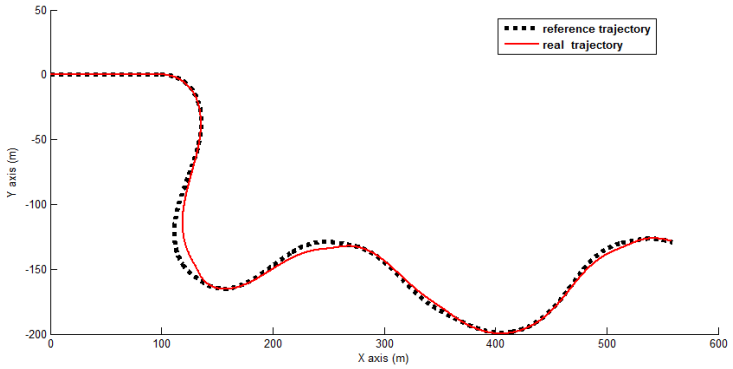

Fig. IV.20: The reference trajectory and the real trajectory at $Vx = 50m/s$ and the prediction horizon at $T = 0.3s$

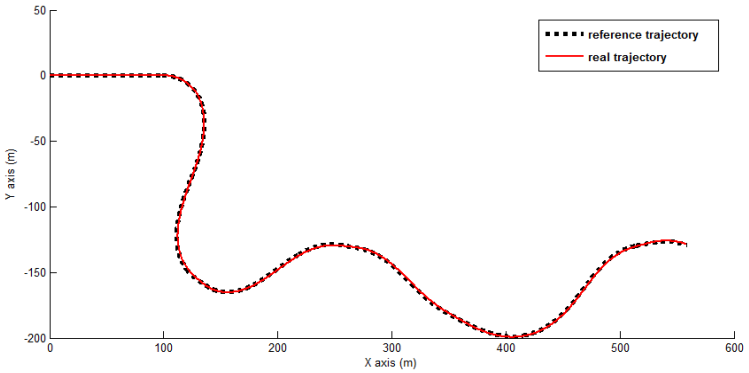

Fig. IV.21: The reference trajectory and the real trajectory at $Vx = 50m/s$ and the prediction horizon at $T = 0.1s$

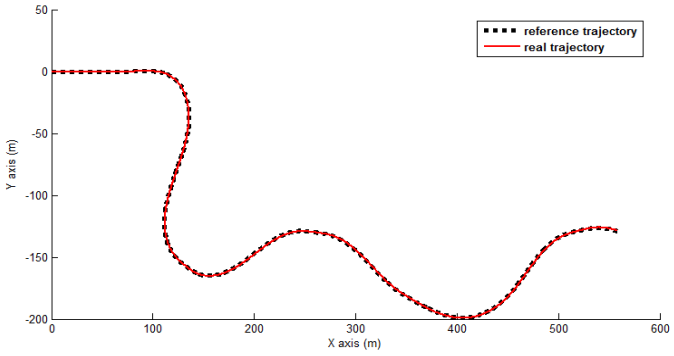

Fig. IV.22: The reference trajectory and the real trajectory at $Vx = 50m/s$ and the prediction horizon at $T = 0.07s$

✠ The error between system inputs and output values (the yaw angle ψ, the position X and Y) at velocity $Vx = 50m/s$ is shown in the following figures respectively:

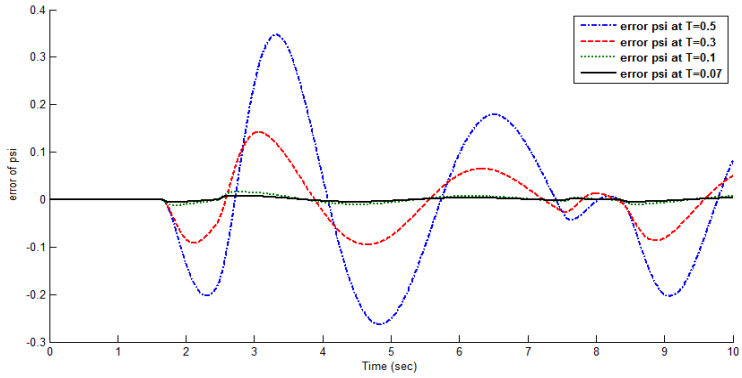

Fig. IV.23: The error between the reference yaw angle ψ and the real yaw angle at $Vx = 50m/s$

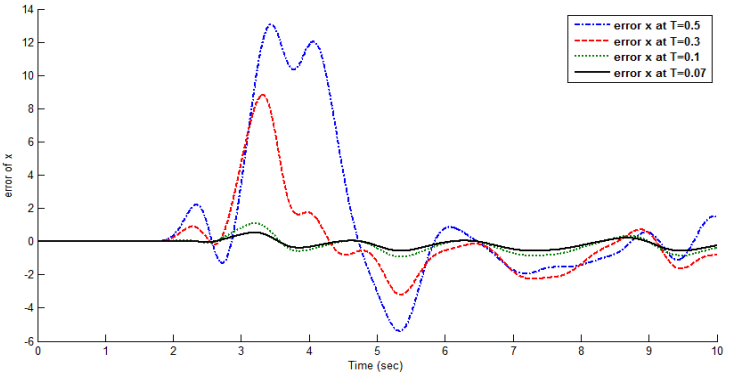

Fig. IV.24: The error between the reference position X and the real position X at velocity $Vx = 50m/s$

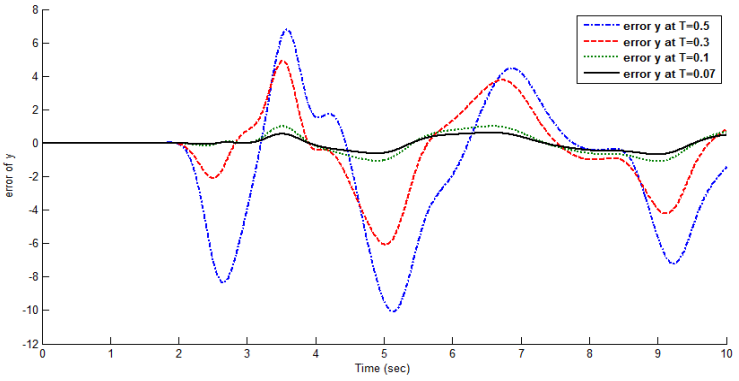

Fig. IV.25: The error between the reference position Y and the real position Y at velocity $Vx = 50m/s$

• The following figures present the control applied to the system inputs (the front and rear steering angles δ_f and δ_r) in different prediction horizons.

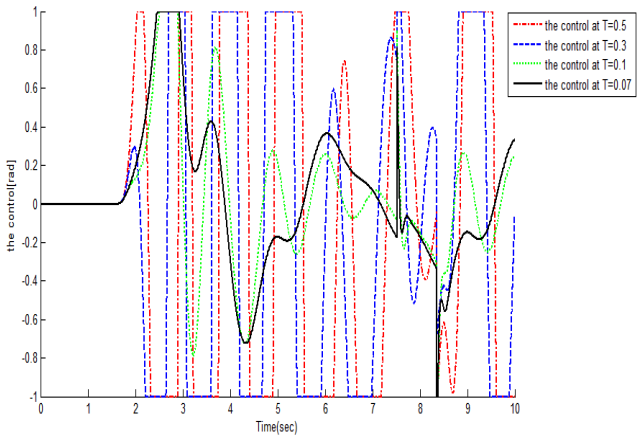

Fig. IV.26: The control applied on the fw

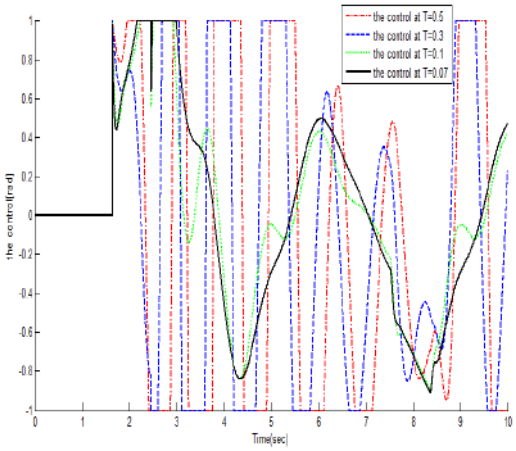

Fig. IV.27: The control applied on the rw

IV.4 Results interpretation

The control law was tested by give different velocity values to the vehicle and different prediction horizon rates, we started by setting the velocity at 10m/s and we changed the prediction horizon by descending values.

At velocity $Vx = 10m/s$ and the prediction horizon at $T = 1s$ as shown in fig (IV.1), the black Curve present the reference trajectory, while the red Curve present the real trajectory of the vehicle ,and as is apparent that the real trajectory doesn't follow the reference properly.

At velocity V= 10m/s and the prediction horizon at $T = 0.7s, T = 0.5s$ and $T = 0.3s$ as shown in fig (IV.2), fig (IV.3) and fig (IV.4) respectively, as it note that the real trajectory started to follow the reference little by little, where we stopped when we reached a very acceptable result, especially in the yaw angles, we noticed that whenever we reduce the prediction horizon we get best results in tracking trajectory, the best example at this stage is at prediction horizon $T = 0.3s$ shown in the fig(IV.4) .

We support these observations by the results of the error calculated between the output and the target, where fig (IV.5), shows the error between the real yaw angle of the vehicle and the calculated angle; that wherever we reduce the prediction horizon the error is reduced. The same observations still correct with coordinates (x, y) shown in fig(IV.6) fig(IV.7) respectively.

We observed that at the velocity $Vx = 10m/s$ and the prediction horizon $T = 0.3s$, the control signal has improved, where the frequency level has decreased and become more smooth, and it is applicable, as observed in the fig (IV.8) and (IV.9).

We change the velocity to $Vx = 30m/s$ and keep it for prediction horizons $T = 0.7s, T = 0.5s, T = 0.3s$ and $T = 0.1s$ as shown in the fig(IV.10), fig(IV.11), fig(IV.12)and fig(IV.13), we notice that is the same previous performance, which whenever we reduce the value of the prediction horizon we get an improvement in the performance of the real trajectory.

The noticeable thing at this stage is that at the prediction horizon $T = 0.3s$, is no

longer enough to reach the best result in tracking the reference.

We support these observations by the results of the error calculated between the output and the target, shown in fig(IV.14) ,fig(IV.15) and fig (IV.16)respectively , where we notice that at the prediction horizon $T = 0.3s$ the error is great while that at $T = 0.1s$ the error became small.

We observed that at the velocity $Vx = 30m/s$ and prediction horizon $T = 0.1s$, the control signal has improved and gave a better result compared to other prediction horizons, where the frequency level has decreased and become more smooth, which is applicable, as shown in the fig (IV.17)and (IV.18).

At last, we tested the control law in high velocity Vx=50m/s and at prediction horizons $T = 0.5s, T = 0.3s, T = 0.1s$ and $T = 0.07s$ as shown in the fig(IV.19),fig(IV.20),fig(IV.21)and fig(IV.22),and also the results are leading to the same judgment, but the noticeable thing is that at prediction horizon T=0.1s we can achieve the tracking trajectory in slower or speeder velocity ,in verifiable way ,and we don't need more than that to get the a good performance in tracking trajectory .

We can verify the observations through the calculated error results between the output and the target shown in fig(IV.23), fig(IV.24) and fig(IV.25) , where at the velocity Vx=50 we observe that at the predictive horizon $T = 0.1s$ and $T = 0.07s$ the error is small ,and noticeable thing is that the error in those predictive horizon values is very similar ,that is mean we don't need more than $T = 0.1s$ as an ideal prediction horizon in order to get best result in tracking trajectory .

The observable thing that at the speed of $Vx = 50m/s$ and the prediction horizons $T = 0.07s$ and $T = 0.1s$, the control signal improved and gave a very close result in these two horizons, where the frequency level decreased and became smoother, and as is noted that the control is applicable as shown in fig(IV.26)and (IV.27).

IV.5 Performance Test

In this test, we tested the control law in different cases than the previous cases. This test is to change the coordinates of the starting point of the vehicle, and the vehicle will start from a location different from the starting point of the reference path.

The first test: At a velocity $Vx = 10m/s$ we changed the position of the vehicle from zero(x=0,y=0) to(x=0,y=5), and the result is that we got good tracking after a small distance from the starting as shown in the figure (IV.28).

The second test: We decided to increase the difficulty of the test, where we raised the velocity to$Vx = 30m/s$ and changed the starting position of the vehicle in both axis X and axis Y where the coordinates became (x=5, y=10) as shown in the figure (IV.31).

Once again, the result was satisfactory, although it took a considerable distance to reach a good tracking, but in the end, the obtained track was consistent with the reference track.

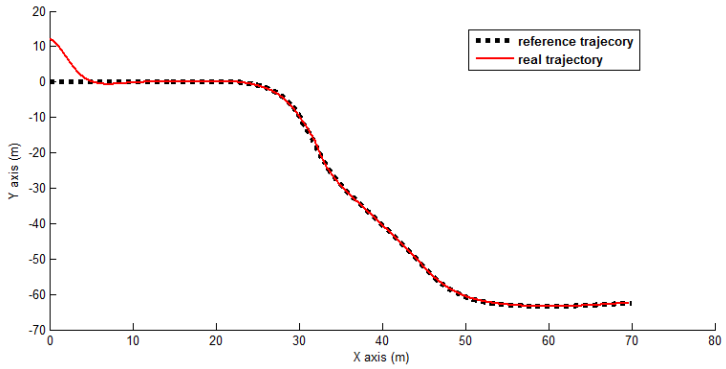

Fig. IV.28: The reference trajectory and the real trajectory at a different starting point at $Vx = 10m/s$

• The following figures present the control applied to the system inputs (the front and rear steering angles δ_f and δ_r) at velocity 10m/s and the starting coordinates are different to zero.

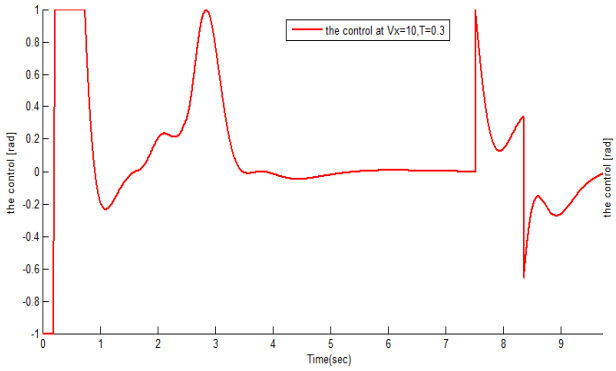

Fig. IV.29: The control applied on the fw

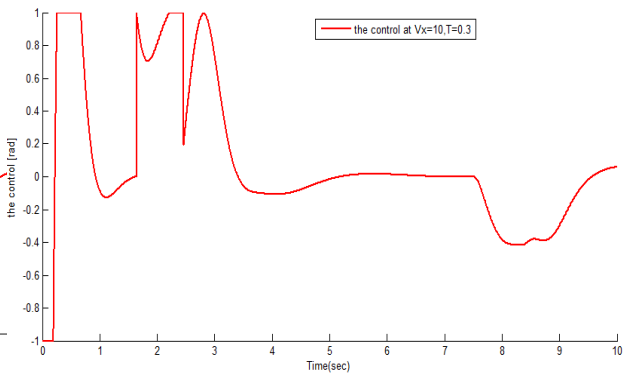

Fig. IV.30: The control applied on the rw

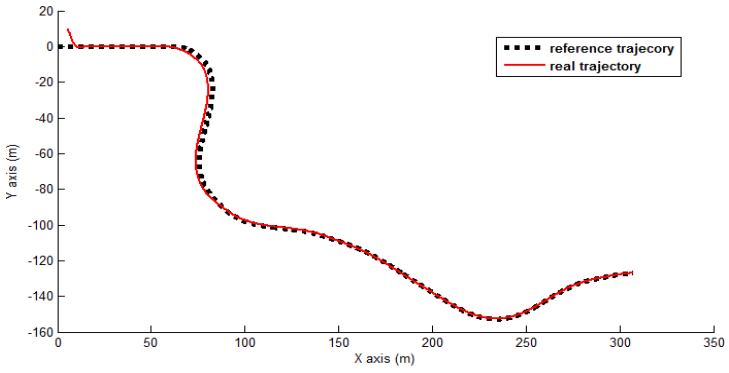

Fig. IV.31: The reference trajectory and the real trajectory at a different starting point at $Vx = 30m/s$

• The following figures present the control applied to the system inputs (the front and rear steering angles δ_f and δ_r) at velocity 30m/s and the starting coordinates are different to zero.

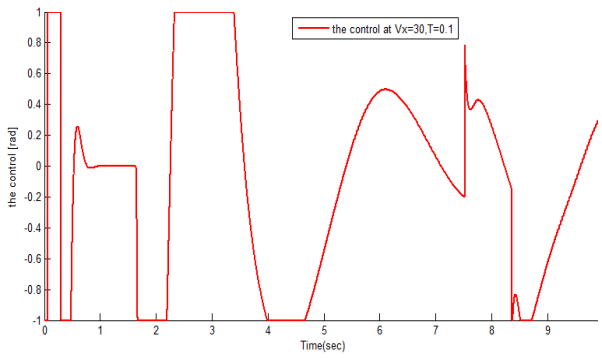

Fig. IV.32: The control applied on the fw

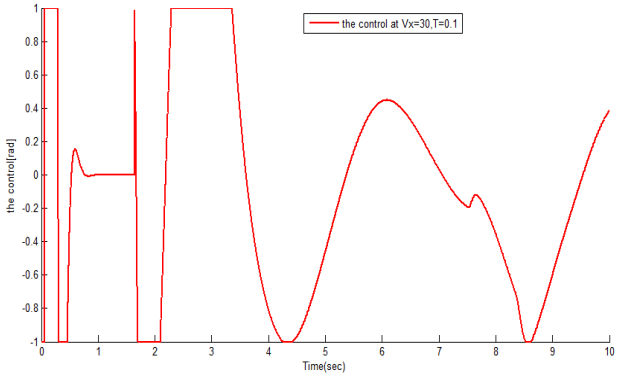

Fig. IV.33: The control applied on the rw

The third test: we changed the reference path again, we set the velocity at Vx = 10 m/s and T=0.1s, and we changed the starting position of the vehicle in both axis X and axis Y and we obtained a very perfect result, where the real path was consistent with the reference track.as shown in figure (IV.34) and (IV.37)

Once Again, the result was satisfactory, thus demonstrating the effectiveness of "Non-linear Continuous-time Generalized Predictive Control" (NCGPC) on nonlinear systems.

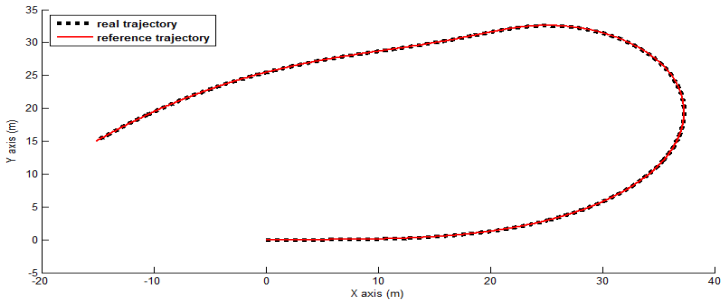

Fig. IV.34: The reference trajectory and the real trajectory at $Vx = 10m/s$ and the prediction horizon at $T = 0.1s$

• The following figures present the control applied to the system inputs (the front and rear steering angles δ_f and δ_r) in the new trajectory .

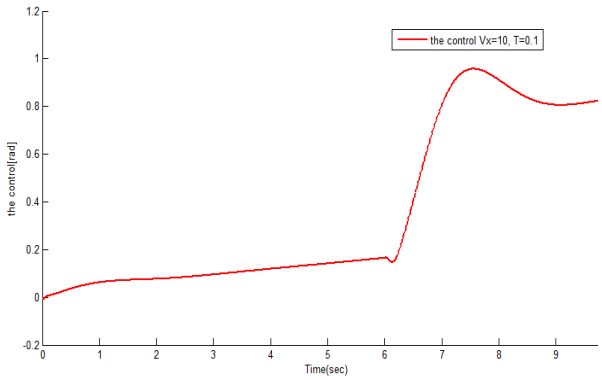

Fig. IV.35: The control applied on the fw

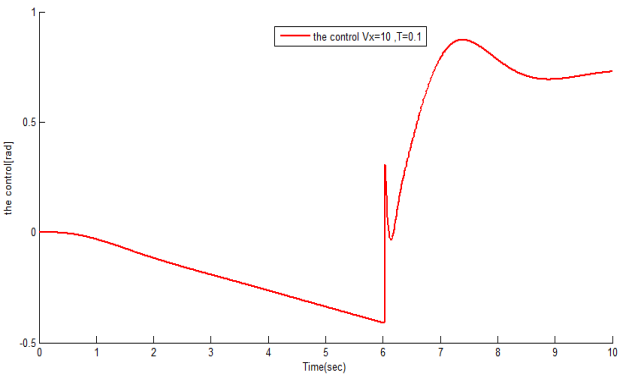

Fig. IV.36: The control applied on the rw

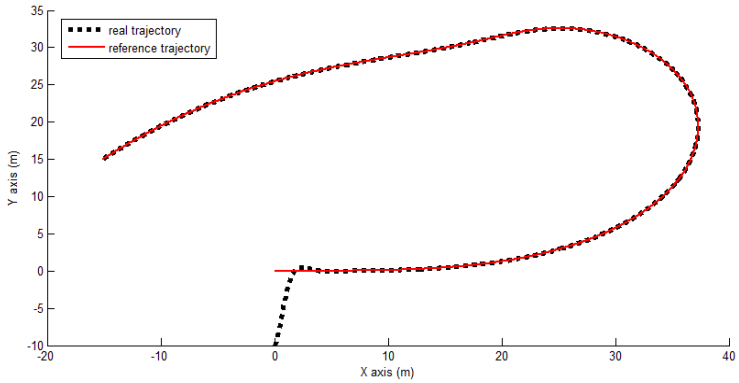

Fig. IV.37: The reference trajectory and the real trajectory at a different starting point at $Vx = 10m/s$

•The following figures present the control applied to the system inputs (the front and rear steering angles δ_f and δ_r)in the new trajectory and the starting coordinates are different to zero.

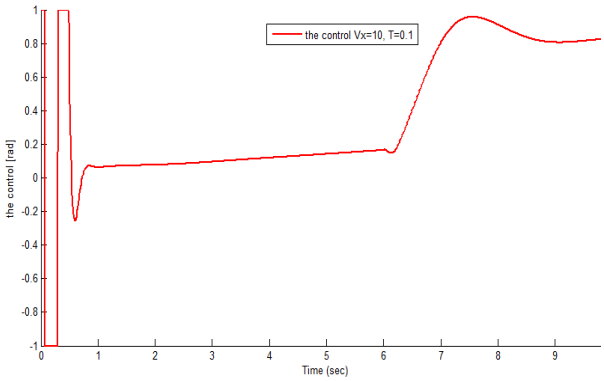

Fig. IV.38: The control applied on the fw

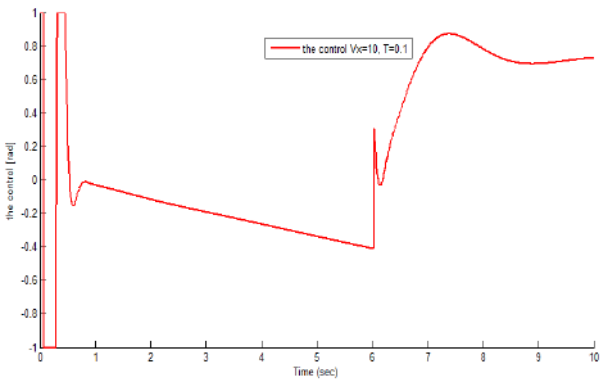

Fig. IV.39: The control applied on the rw

• As a result, robot testing results at low speeds, high speeds, and very high velocities have yielded very satisfactory results compared to the system type, where is considered as a dynamic system, which is difficult to control at high speeds, off-road and slippery.

In the performance test, although the initial values of the robot site coordinate changed, it was able to follow the reference path. Similarly, when we change the reference path was changed, the controller does not found it difficult to follow the new path, and without any complicated procedures.

Performance test results provided clear evidence of NCGPC's strength, that this approach is able to follow a new path also, with high accuracy, with the same previous control, without any changes. This shows that the NCGPC approach is strong and adapted to the various changes of systems.

IV.6 Conclusion

In this chapter, we have introduced a direct application of the nonlinear continuous-time generalized predictive control (NCGPC) in a multi-input and output system (MIMO).

The control law has been synthesized to fit the controlled system; this system is a model of a mobile robot vehicle type with four wheels.

The results of the simulation tests on the system were presented, where the control law was tested in tracking a given trajectory, those tests were at a different velocity of the vehicle and different predictive horizon values.

The performance of this law was also tested in difficult situations. The results of all these tests were interpreted and presented in curves.

The results of the error measured between the system outputs (ψ ,X,Y), and the target were analyzed and presented in curves.

At the last, these results allowed us to judge the nonlinear continuous-time generalized predictive control (NCGPC) approach, where we can say that the approach of (NCGPC) is strong in tracking the target; the results of tracking a path of robot vehicle type were the witness on that.

General conclusion and perspectives

The purpose of this work was to apply the Control law, which allows the tracking of a reference path applied to a multi-input and output system.

The controlled system is the mathematical model of a mobile robot car-type(RobuFast-A), which is considered as a non-linear system with a multi-input and output, so it is more appropriate to apply the non-linear continuous-time generalized predictive control (NCGPC) on this system.

Generalized prediction control, which is based on the predictive process as a principle of work, where it can predict the future behavior of the system, this feature provides a smooth tracking of system changes.

Reaching the goal was through the stages:

Initially, the robot was modeled with the kinematic model, where the bicycle model replaced the vehicle model. The robot is also modeled in a dynamic model that describes the dynamic behavior of the robot, which takes into account the wheel slippage at turns and the difficulty of controlling at high speeds.

The predictive control model has been developed to fit the multi-input and output system; mathematical tools were used to facilitate the modeling of the control law. The calculation of the error between the system inputs and the outputs, and the calculation of the performance index, are important in applying the generalized prediction control approach.

The control law is synthesized before testing, the simulation test of the control law through its applying on the vehicle model, provided satisfactory results in tracking a reference path.

The control law was tested at different velocities of the vehicle and at various predictive horizons, Were, we increase the velocity by steps, from slow to high speed.

The performance of this law was tested in difficult situations; were the initial coordinates of start point and the reference trajectory were changed.

The results obtained showed the strength of the NCGPC in tracking a particular path, the results were very satisfactory.

The results of the performance test provided clear evidence of the strength of the NCGPC. Although the initial values of the robot position coordinates were changed, it was able to follow the reference path. This approach was able to follow a new path as well, with high accuracy, with the same former control and without any changes.

This shows that the NCGPC approach is robust and adapts to the different changes of systems.

The field of predictive control is a largely alive field and many contributions are regularly presented, which also indicates many perspectives.

With regard to this work, some proposals seem interesting for continuity:

• Incorporate the predictive control with artificial intelligence techniques.

• Expand the application of the generalized predictive control to real cars rather than robots.

Bibliography

[AGN08] Coelhon dos Santos André Guilherme Nogueira. *"Autonomous Mobile Robot Navigation using Smartphones"*. Mémoire de Magister ,Instituto Superior Técnico, Universidade Técnica de Lisboa, 2008.

[Ahm15] Bengoufa Ahmed. *"La commande prédictive des systèmes linéaires Multi variables"*. Mémoire du Master ,Université Djilali Bounaama,Khemis Miliana, 2015.

[Ben10] Larafi Bentouhami. *"Controle de la Dynamique Latérale d'un Véhicule avec Estimation des Forces de Contact Roue–Sol"*. Mémoire de Magister, Université de Batna, 2010.

[Bez13] Abdallah Bezzini. *"Commande Prédictive Non Linéaire en Utilisant Les Systèmes Neuro-Flous et les Algorithmes Génétiques"*. Mémoire de Magister ,Université Mohamed Khider – Biskra, 2013.

[BOU11] OUASSILA BOUREBIA. *"Commande Prédictive Floue des Systèmes Non Linéaires"*. thése Doctorat , université mentouri de constantine, 2011.

[CEF04] C. Bordons Camacho E. F. *"Model predictive control"*. Ed. Springer-Verlag, London, 2004.

[Dab10] Marcelin Dabo. *"Commande prédictive généralisée non linéaire à temps continu des systémes complexes"*. thése de Doctorat ,Université de Rouen, 2010.

[ELB08] D. Salle E. Lucet, C. Grand and P. Bidaud. *"Stabilization algorithm for a high speed car-like robot achieving steering maneuver."*. In IEEE International Conference on Robotics and Automation (ICRA), pages 2540–2545, Pasadena, California (USA)., 2008.

[FIL16] David FILLIAT. *"Robotique Mobile"*. École Nationale Supérieure de Techniques Avancées ParisTech, Dernière mise à jour : 17 octobre 2016.

[Gio09] L Giovanini. *"Predictive feedback control: an alternative to proportional–integral–derivative control"*. Universidad Nacional del Litoral, Ruta nacional 168, Paraje El Pozo (CC 127), Santa Fe,Argentina, 2009.

[KC15] Matthew Kroh and Sricharan Chalikonda. *"Essentials of Robotic Surgery"*. Springer International Publishing Switzerland, 2015.

[KM01] M. Katebi and M. Moradi. *"Predictive PID controllers"*. IEE Proc. Control Theory Appl., 2001.

[KP04] K. Kozlowski and D. Pazderski. *"Modeling and control of a 4-wheel skid-steering mobile robot"*. International journal of applied mathematics and computer science, 2004.

[Kri12] Mohamed Larbi Krid. *"Commande en suivi de chemin et en roulis des robots mobiles rapides en présence de glissements et d'instabilités"*. thése de doctorat ,l'Université Pierre et Marie Curie - UPMC L'école doctorale Sciences Mécaniques, Acoustique, Electronique et Robotique de Paris, 2012.

[LCI99] A. De Luca L. Caracciolo and S. Iannitt. *"Trajectory tracking control of a four-wheel differentially driven mobile robot."*. In Proceedings of the IEEE International Conference on Robotics and Automation, pages 2632–2638, Detroit, Michigan, May 1999.

[LCO02] T. Leo L.M. Corradini and G. Orlando. *"Experimental testing of a discrete-time sliding mode controller for trajectory tracking of a wheeled mobile robot in the presence of skidding effects."*. Journal of Robotic System, 2002.

[Lss01] *"chapter I Introduction to Control Systems"*. prentice hall upper saddle river nj, 2001.

[R01] Burns R. *"Advanced Control Engineering"*. Linacre House, Jordan Hill, Oxford,, 2001.

[Raj12] Rajesh Rajamani. *"Vehicle Dynamics and Control/Second Edition"*. Springer New York Dordrecht Heidelberg London, 2012.

[Ås02] Karl Johan Åström. *"Control System Design"*. University of California Santa Barbara, 2002.

[San99] Ben-Zion Sandier. *"ROBOTICS,Designing the Mechanisms for Automated Machinery"*. Academic Press, 1999.

[sm09] salima meziane. *"commandes Adaptative et prédictive du la machine Asynchrone"*. thése de Doctrate ,université mentouri de constantine, 2009.

[SNZ10] Syed Salim Syed Najib and Maslan Zainon. *"Control Systems Engineering"*. Technical University of Malaysia Malacca, 2010.

[Sol07] Appin Knowledge Solutions. *"Robotics"*. INFINITY SCIENCE PRESS LLC Hingham, Massachusetts New Delhi, 2007.

[Tza14] Spyros G. Tzafestas. *"Introduction to Mobile Robot Control"*. School of Electrical and Computer Engineering National Technical University of Athens Athens, Greec, 2014.

[Wan08] Ye Z. Cai W.-J and Hang C.-C Wang, Q.-G. *"PID Control for multivariable processes"*. Springer-Verlag, 2008.

Annex

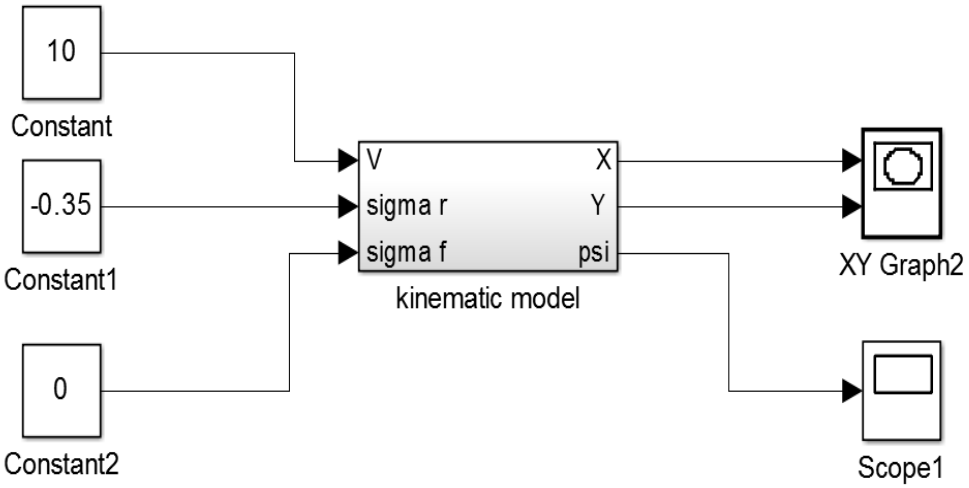

Fig. 40: Block diagram of kinematic model

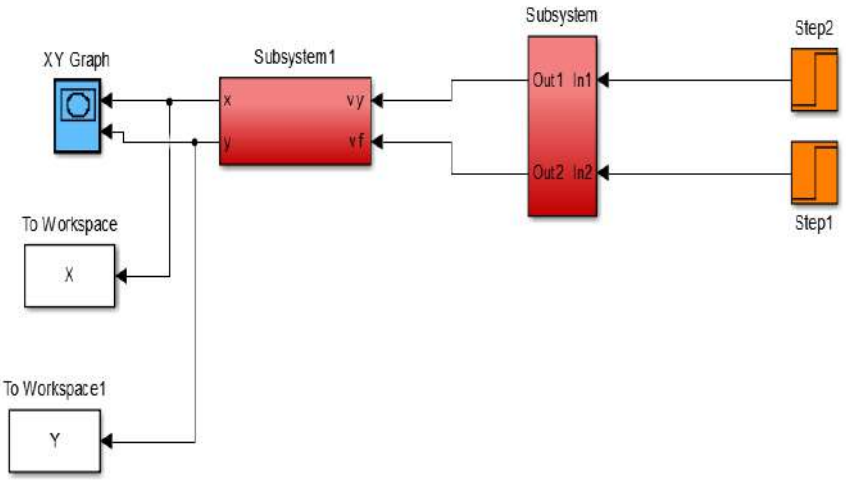

Fig. 41: Block diagram of dynamic model

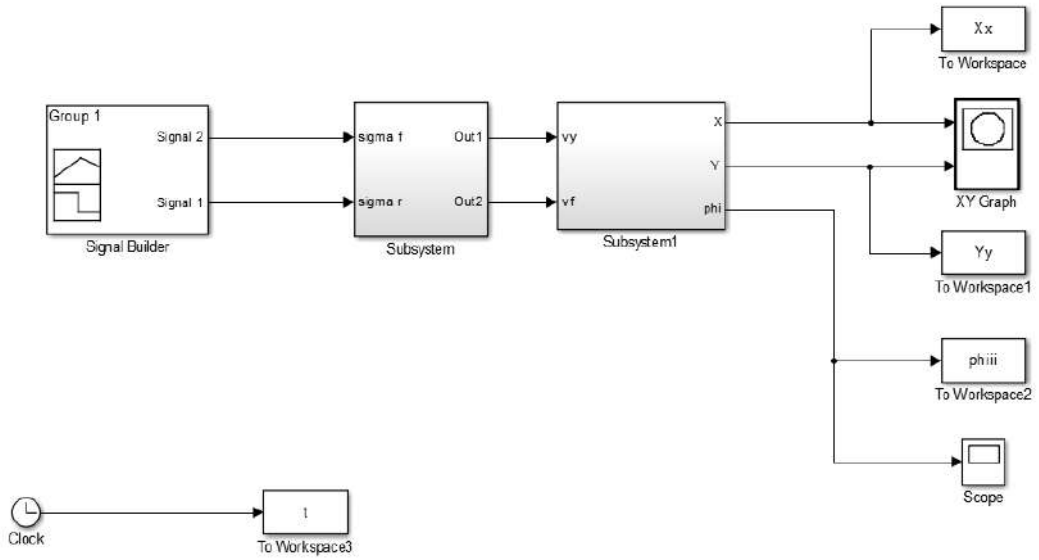

Fig. 42: the block of the reference trajectory

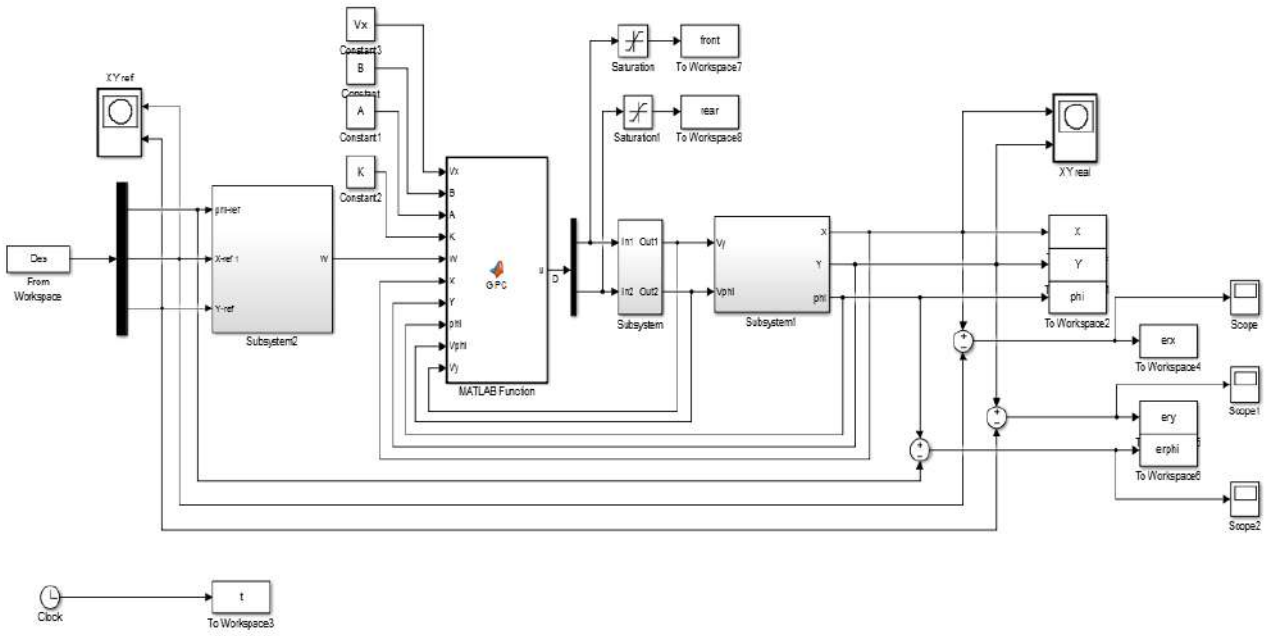

Fig. 43: the block of the control applies to the system

الملخص

الروبوتات المتنقلة تشمل تطبيقات متعددة، تعمل الروبوتات المتنقلة في الهواء الطلق في بيئات متنوعة ، في هذا العمل نحن مهتمون بتصميم وحدة تحكم لروبوت متنقل سريع في الهواء الطلق ، والذي يسمح للروبوت بالتحرك في بيئة طبيعية بسرعة عالية وتتبع مسارًا مرجعيًا.تم تطوير النموذج الديناميكي ، والذي يأخذ في الاعتبار انزلاق العجلات ، ويعتبر شرطًا هامًا في عملية النمذجة ، يتم استخدام إسقاط وضع السيارة في نظام الإحداثيات المطلق لتحديد النموذج الحركي.

نقدم نهجًا جديدًا لحل مشكلة تتبع المسار من خلال تطبيق التحكم التنبئي المعمم غير الخطي المتواصل .(NCGPC) جهاز التحكم يعتمد على النموذج الديناميكي للمركبة . يسمح نموذج التنبؤ بتوقع السلوك المستقبلي للنظام وفقًا للقيود الديناميكية للنظام .أظهرت نتائج المحاكاة دقة كبيرة في التحكم والقوة في تتبع المسار مع القدرة على التعامل مع التغيرات في البيئة وحالة الروبوت ، مما يعني أن هذا النهج قوي.

كلمات مفتاحية: روبوت متحرك، تتبع مسار، تحكم تنبؤي معمم مستمر غير خطي، نمذجة.

abstract

Mobile robots include multiple applications, outdoor mobile robots work in varied environments, In this work, we are interested in designing a controller of fast outdoor mobile robots, which allows the robot moving in a natural environment with a high speed and tracking a reference trajectory.The dynamic model was developed, which take into account sliding of the wheels, and is considered an important condition in the modeling process, the projection of the vehicle position in the absolute coordinate system is used to define the kinematic model.We present a new approach to solving a tracking path problem by applying nonlinear continuous-time generalized predictive control (NCGPC). The controller is based on the dynamic model of the vehicle. The prediction model allows anticipating the future behavior of the system according to the dynamic constraints of the system. The simulation results showed great accuracy in control and strength in track tracing with the ability to cope with changes in the environment and the condition of the robot, which means that this approach is robust.

Keywords: Mobile robot**,** Path tracking**,** Non-linear Continuous-time Generalized Predictive Control**,** Modeling**.**

Résumé

Les robots mobiles incluent des applications multiples, les robots mobiles extérieurs travaillent dans des environnements variés, dans ce travail nous sommes intéressés par la conception d'un contrôleur de robot mobile extérieur rapide qui permet au robot de se déplacer dans un environnement naturel à haute vitesse.Le modèle dynamique a été développé, qui prend en compte le glissement des roues, et est considéré comme une condition importante dans le processus de modélisation, la projection de la position du véhicule dans le système de coordonnées absolues est utilisée pour définir le modèle cinématique.Nous présentons une nouvelle approche pour résoudre un problème de chemin de suivi en appliquant une commande prédictive généralisé non linéaire en temps continu (NCGPC).Le contrôleur est basé sur le modèle dynamique du véhicule.Le modèle de prédiction permet d'anticiper le comportement futur du système en fonction des contraintes dynamiques du système.Les résultats de simulation ont montré une grande précision dans le contrôle et la force dans le traçage de piste avec la capacité de faire face aux changements dans l'environnement et l'état du robot, ce qui signifie que cette approche est robuste.

Mots-Clés : Robot mobile**,** suivi de trajectoire**,** commande prédictive généralisé non linéaire en temps continu**,** modélisation**.**